Available online at www.sciencedirect.com
ScienceDirect
Geochimica et Cosmochimica Acta 73 (2009) 5918–5943
Geochimica et Cosmochimica Acta
www.elsevier.com/locate/gca

Siderophile and other geochemical constraints on mixing relationships among HED-meteoritic breccias

Paul H. Warren *, Gregory W. Kallemeyn, Heinz Huber [1], Finn Ulff-Møller, Wonhie Choe

Institute of Geophysics, UCLA, Los Angeles, CA 90095-1567, USA

Received 7 July 2008; accepted in revised form 23 June 2009; available online 12 July 2009

Abstract

We have used neutron activation and electron-probe fused-bead techniques to analyze the bulk major and trace-element compositions of 104 named HED meteorites (about 100–102 distinct meteorites, depending upon pairings), including 32 polymict eucrites, 30 howardites and six diogenites. Most were not previously analyzed for siderophile trace elements; many not even for major elements. Our typical sample was ~350 mg, and in some cases two separate chips were analyzed as a test of meteorite heterogeneity. Meteorites with extraordinary compositions include Bluewing 001, an unequilibrated eucrite that is rich in Ti, Sm and other incompatible elements; Y-791192, a cumulate-dominated polymict eucrite; and LEW 87002, an oddly Sm-rich howardite dominated by a ferroan variety of diogenite. The eucrite:diogenite mixing ratio is the single most important factor determining the compositions of polymict HEDs, but wide ranges in eucrite incompatible element contents, in diogenite Cr and V contents, and in Sc contents of both eucrites and diogenites, make for diversity among the polymict HEDs.

As our new siderophile data help to show, the common practice of describing the entire class of howardites as regolith breccias is erroneous. Most howardites are fragmental breccias showing no sign of origin from true (in the lunar sense, i.e., soil-like) near-surface regolith. Howardites are highly diverse in Ni content, often remarkably Ni-poor, compared to lunar regolith breccias. However, the few (8) howardites with between 300 and 1200 μg/g Ni consistently show some combination of other traits suggestive of regolith origin. Most importantly, all four cases (or five if we include Malvern, which appears to have been altered by annealing) of howardites known to have enrichments in solar-wind noble gases belong to the >300 μg/g Ni group. In many cases, an abundance of glasses, particularly in spheroidal or turbid-brown form, provides additional evidence for regolith origin. We propose that the important subset of howardites that are regolith breccias be formally distinguished by the designation regolithic howardite.

Apart from high siderophile levels, the regolithic howardites are compositionally distinctive in having Al_2O_3 consistently near 8–9 wt%; corresponding to a eucrite:diogenite mixing ratio of precisely 2:1. Assuming the HEDs are reasonably representative of the ancient (i.e., pre-vestoid-launch) surface of Vesta, this clustering of regolith composition is difficult to explain unless most of the ancient diogenite component was brought to the surface in a single early episode (i.e., probably a single great impact), after which smaller-scale cratering (with no further major excavations of diogenite until the vestoid-forming event), efficiently homogenized the surface. Such a single-excavation model may also help to explain why diogenites, in marked contrast with eucrites, are seldom polymict; and why Al_2O_3-poor (diogenite-dominated) howardites consistently lack major siderophile enrichments. The low siderophile contents of polymict eucrites are most enigmatic. Possibly in the HED-asteroidal context (low collision velocities, etc.), only materials blended by multiple impacts consistently acquire major enrichments in siderophile elements.

* Corresponding author. Tel.: +1 310 825 3202; fax: +1 310 206 3051.
E-mail address: pwarren@ucla.edu (P.H. Warren).
[1] Present address: RJ Lee Group, Inc., 2600N. 20th Ave., Pasco, WA 99301, USA.

0016-7037/$ - see front matter © 2009 Elsevier Ltd. All rights reserved.
doi:10.1016/j.gca.2009.06.030

1. INTRODUCTION

In many respects, the HED (howardite + eucrite + diogenite) meteorites represent the most extensive sampling of any differentiated extraterrestrial body. The late-2008 Meteoritical Bulletin database (maintained by J.N. Grossman on the official society web page) lists 819 HEDs with officially sanctioned names. The total mass of these 819 stones, 1147 kg, is nearly three times the mass of all lunar samples (382 kg Apollo + 0.2 kg Luna + 46 kg meteoritic) and 12 times the combined total mass (94 kg) of the current set of 75 officially named martian stones. Most HEDs (80–90%) are impact breccias, and about half of the breccias are manifestly polymict. To a zeroeth approximation, the unmixed igneous materials represented by unbrecciated and monomict-brecciated HED samples are limited to just two compositionally/mineralogically narrow types: eucrites and diogenites. However, no consensus exists concerning the way two such disparate igneous materials (basalt vs. nearly pure orthopyroxenite) came to dominate the exterior portion of an asteroid on which compositional diversity is essentially limited to these two materials and impact-mixture between them. All 172 howardites are obviously polymict, eucrite + diogenite, breccias. Only eight of the 182 named diogenites are polymict breccias (virtually all the rest are monomict breccias). But over half of the 465 named eucrites are brecciated, including 140 that are manifestly polymict.

The HED asteroid (Vesta?; Binzel and Xu, 1993) experienced cratering, impact-mixing, and megaregolith/regolith development analogous to the processes that pervasively altered the chemistry and structure of the upper crust of the Moon. However, for neither body is this impact processing understood in detail, and the analogy is complicated (or in a sense, made more interesting) by the factor of (at least) 200 mass difference between the two bodies, while impact velocities are much smaller (by a factor of ~3) in the asteroid belt (Farinella and Davis, 1992). In this study, we provide a substantial augmentation to the previous database of bulk-compositional data for HEDs, including in many cases determination of highly siderophile elements such as Ni and Ir, which constrain the proportion of chondritic matter admixed with eucritic and diogenitic debris within the breccias. These data provide new statistical constraints on the style of impactor debris admixture, and also on subtle but revealing aspects of the diversity of the basaltic, gabbroic and orthopyroxenitic components that were mixed to form the polymict breccia variation trends.

Thanks to a sampling that is both well-contextualized and extensive, the best understood suite of impact-blended extraterrestrial material comes from the Moon (Apollo and Luna documented samples, augmented, in recent years, by numerous meteorites). The most extensively impact-gardened lunar samples are the "mature" regoliths, including some lunar-meteoritic regolith breccias. One of the goals of this study is to examine the degree to which the howardites are analogs of the lunar regolith samples. Mature lunar regolith samples have several diagnostic characteristics. They tend to contain high contents of solar-wind implanted noble gases (e.g., McKay et al., 1986, 1991), and an abundance of tiny quenched melt-droplet spheroids (e.g., Delano et al., 2007). Although scatter among the data makes for a less useful gauge of regolith maturity, siderophile enrichments are another characteristic of regolith-processed material (Warren, 2004).

2. SAMPLING AND EXPERIMENTAL METHODS

Most of our samples were selected to provide a large set of brecciated HEDs, random except for avoiding meteorites whose bulk compositions were already well determined by previous studies, or that appear severely weathered. However, a large minority of our samples (most of those in Table 1) were selected for the purpose of gauging diversity among HEDs described as igneous or monomict-brecciated (but distinguishing monomict- vs. polymict-brecciated HEDs is not always easy; one purpose of our analyses is to provide siderophile constraints on the mixing issue). The analyzed samples were intended to be representative of each bulk meteorite. In a few cases clasts (or otherwise distinctive domains) were also analyzed, but those results will be published elsewhere. Two partial exceptions are Millbillillie, where our samples represent three distinct textural domains (CG = coarse-grained, FG = fine-grained, FD = fine-grained and dark), and likewise NWA 1182 (we studied light-matrix and dark-matrix chips). But these different domains are roughly similar in composition, and we assume that collectively they are representative of the bulk rock. Sample masses were generally >200 mg and average (per meteorite, not per analysis) 500 mg. Sources of samples are listed in Tables 1–3. In two cases, we analyzed aliquots from large-mass powders prepared elsewhere: the ALH 77256 diogenite and the Chaves howardite.

In most cases, the first step was to crush the sample to a fine powder using an agate mortar and pestle. A small (typically 15–25 mg) aliquot of each powder was removed for determination of major and minor elements (Na, Mg, Al, Si, K, Ca, Ti, Cr, Mn and Fe) by the technique of microprobe fused bead analysis (MFBA). The MFBA powders were fused on Mo foil strips in an Ar-flushed atmosphere, and the glasses were analyzed using UCLA's JEOL JXA-8200 electron probe or its UCLA predecessor, a Cameca CAMEBAX. MFBA analyses were run at conventional probe settings, i.e., accelerating voltage of 15 KV, focused beam, and count durations of 15–20 s for most elements (except 5–8 s for K and Na, but for these elements we essentially ignore the MFBA results in favor of their INAA counterparts). For the feldspar-poor diogenites, obtaining a representative glass can be problematical (Beck et al., 2009). We fluxed our diogenite powders by mixing with 1/3 as much mass of a standard rock powder of K-feldspar composition (JF-2: Govindaraju, 1994), performed MFBA, and solved for the diogenite composition by subtracting out the JF-2 component. This added step has minimal impact on net precision for Mg, Si, Ca, Ti, Cr, Mn and Fe (except for Si these elements are at extremely low concentration in JF-2), but it does render the MFBA highly imprecise for Al (i.e., for Al in diogenites we rely almost exclusively on INAA). The JXA-8200, with conventional settings, was also used in some cases to acquire thin-section mineral anal-

Table 1
Bulk-rock compositional results for 22 elements in 25 noncumulate eucrites, nine cumulate eucrites and six diogenites. For additional elements and itemization of uncertainties, see the Electronic Annex.

	Sample[a]	Weathering	Mass	Source	Na_2O (wt%)	MgO (wt%)	Al_2O_3 (wt%)	SiO_2 (wt%)	CaO (wt%)	MnO (wt%)	FeO (wt%)	Sc (μg/g)	Ti (mg/g)	V (μg/g)	Cr (mg/g)	Co (μg/g)	Ni (μg/g)	Ga (μg/g)	Sr (μg/g)	Ba (μg/g)	La (μg/g)	Sm (μg/g)	Eu (μg/g)	Lu (μg/g)	Hf (μg/g)	Ir (pg/g)
Noncumulate eucrites: unbrecciated (1–10), brecciated-monomict (11–22), or brecciated with mixing state uncertain (23–25)																										
1	Agoult	W1	555	Farmer	0.404	6.84	11.88	49.65	9.81	0.49	19.33	30.2	3.2	62	2.11	6.3	6[c]	1.48	71	31	2.46	1.50	0.56	0.24	1.03	<1500
2	Bluewing 001	W1	174	Gessler	0.59	7.21	10.91	50.30	10.22	0.53	18.68	29.3	6.0	75	2.84	8.3	<18	2.26	120	83	6.8	3.7	1.03	0.40	2.52	<1500
3	EET 92004,13	A/B	379	MWG	0.350	6.9	13.4	49.04	10.16	0.55	18.26	27.0	3.1	59	1.94	6.3	<30	1.03		42	2.12	1.27	0.68	0.21	0.87	<3000
4	GRA 98098,31-A	B	434	MWG	0.51	6.65	13.32	49.01	10.24	0.52	18.46	31.5	3.1	45	1.44	4.7	<30	<2	69	45	3.6	1.90	0.64	0.31	1.46	<2000
	GRA 98098,31-B		440	MWG	0.51	6.68	13.20	49.01	10.28	0.53	18.47	31.5	2.8	42	1.45	4.7	<30	<2	69	43	3.6	1.90	0.64	0.31	1.48	<1400
5	LEW 88009,4	A	224	MWG	0.360	6.8	13.0	49.30	10.23	0.56	18.67	28.6	4.0	72	2.12	5.5	<30	0.91		38	2.39	1.61	0.64	0.25	1.15	<3000
6	LEW 88010,5	A	428	MWG	0.449	7.7	11.5	48.95	9.89	0.52	18.83	26.8	6.3		2.62	7.1	2.1	1.11		<60	5.5	3.12	0.81	0.40	2.10	41
7	PCA 91078,10-a	A/B	310	MWG	0.344	7.0	13.1	48.43	10.01	0.55	18.98	25.0	2.9		2.16	6.1	0.22	0.69		25	1.66	1.03	0.56	0.17	0.75	0.79
	PCA 91078,10-b		305	MWG	0.331	7.0	13.1	48.43	10.05	0.56	19.11	26.0	2.6	70	2.25	6.2	<30	0.98		35	1.74	1.08	0.58	0.19	0.77	<3000
8	PCA 91245,11-a	B	323	MWG	0.398	7.12	13.39	48.49	10.05	0.53	18.93	27.2	2.4	80	2.51	6.4	<30	1.32	78	<70	1.42	1.00	0.55	0.17	0.69	<2700
	PCA 91245,11-b		327	MWG	0.438	7.16	13.39	48.49	9.97	0.57	19.01	27.1	2.6	87	2.54	6.7	<30	1.33	75	<50	1.53	1.01	0.58	0.17	0.63	<3000
9	QUE 97014,20-A	A	308	MWG	0.419	6.34	13.07	49.33	10.38	0.52	18.86	30.0	4.9	64	2.00	12.5	<11	2.3	75	<60	2.79	1.67	0.65	0.25	1.16	<3500
	QUE 97014,20-B		306	MWG	0.422	6.41	12.57	49.25	10.43	0.50	18.58	29.8	3.8	45	2.04	7.8	9[c]	<3	69	32	3.0	1.82	0.65	0.28	1.35	<1800
10	RKP 80224,6	A	132	MWG	0.449	7.10	13.52	48.47	10.02	0.58	19.13	28.4	3.0	77	2.28	5.1	<59	1.6	70	<50	1.51	0.87	0.73	0.25	0.82	<5000
	RKP 80224,7	A/B	218	MWG	0.449	6.41	13.64	49.08	10.10	0.56	18.27	30.7	2.2	69	2.38	5.8	1.55	1.55	<140	26	2.31	1.30	0.67	0.28	0.97	2.1
11	EET 87542,7	A	306	MWG	0.50	6.74	14.58	48.00	10.26	0.59	18.24	33.0	2.3	59	2.22	6.1	0.25	1.64	79	<40	3.5	2.00	0.72	0.31	1.36	0.42
12	EET 90020,8-a	A	326	MWG	0.410	6.37	12.91	49.36	10.28	0.54	18.48	30.4	4.1	71	2.32	4.55	<10		54	<30	1.28	0.98	0.60	0.22	0.73	<1500
	EET 90020,8-b		332	MWG	0.421	6.43	12.89	49.36	10.27	0.56	18.57	31.4	3.9	67	2.38	4.43	<11	0.66	62	<30	1.37	1.01	0.60	0.23	0.77	<1900
13	LEW 86002,10-A	A/B	375	MWG	0.410	6.84	12.33	48.85	9.70	0.57	19.24	28.1	3.6	66	2.11	6.0	<18	1.32	82	28	1.62	1.02	0.54	0.19	0.90	<1000
	LEW 86002,10-B		400	MWG	0.451	6.38	12.64	49.72	10.06	0.57	18.63	29.5	3.1	64	2.14	5.3	0.47	1.54	66	37	1.75	1.15	0.57	0.21	0.96	0.46
14	LEW 87010,6	A	171	MWG	0.448	6.63	12.85	48.99	9.79	0.61	19.17	31.3	4.0	81	2.38	6.4	0.40	1.48	81	30	2.81	1.60	0.64	0.27	1.01	0.88
15	Millbillillie-A(CG)		148	U. Tokyo	0.49	6.22	12.56	51.37	10.48	0.48	16.32	37.3	5.9	62	1.89	5.2	0.68	1.9	<90	<70	4.2	2.46	0.76	0.39	1.96	1.05
	Millbillillie-B(FD)		222	U. Tokyo	0.355	8.56	10.21	48.69	8.74	0.63	20.54	26.7	4.9	69	2.98	5.6	1.8	1.27	<70	47	4.5	2.49	0.70	0.33	1.88	50
	Millbillillie-C(FG)		164	U. Tokyo	0.430	6.90	12.08	49.73	10.05	0.58	18.81	32.0	4.0	69	2.28	6.4	0.38	1.15	<120	<50	2.8	1.67	0.64	0.27	1.28	4.0
16	Peramiho	fall	483	NM Wien	0.454	6.88	12.01	50.50	10.37	0.53	18.34	33.6	5.0	70	2.05	6.3	9.0	1.34	56	26	3.0	1.85	0.69	0.29	1.36	<1000
17	RKP 80204,14	A	320	MWG	0.414	6.87	12.78	49.21	10.19	0.57	18.54	29.9	4.6	85	2.20	3.91	0.48	1.50	53	24	2.51	1.34	0.67	0.24	1.29	6.5
18	Sioux County	fall	279	UCLA	0.389	7.25	11.88	50.28	9.84	0.58	18.70	30.6	3.5	69	2.21	6.4	<40	1.16	62	50	1.81	1.25	0.48	0.22	1.04	<3000
19	Stannern?	fall	502	NM Wien	0.47	6.10	11.37		10.27	0.49	18.55	29.7	3.9	47	2.16	5.3	<10	<3	74	52	5.3	2.98	0.76	0.40	2.22	<3000
20	Y-791186,88-A		270	NIPR	0.50	7.69	11.59	50.03	9.81	0.56	18.43	28.8	5.3	62	2.73	4.16	0.49	1.01	80	55	3.07	1.82	0.77	0.30	2.04	<2
	Y-791186,88-B		260	NIPR	0.52	7.47	11.16	49.50	10.13	0.54	18.90	30.4	5.3	67	2.97	3.74	<30	1.01	90	61	3.61	2.43	0.79	0.34	2.25	<3000
21	Y-82037,64		372	NIPR	0.387	6.76	13.51	51.00	10.28	0.56	17.24	28.4	1.5	73	2.02	6.4	1.19	<2.6	63	23	2.08	1.33	0.58	0.22	0.97	0.59
22	Y-82202,63		51	NIPR	0.463	6.75	14.29	49.37	10.51	0.56	17.73	27.4	4.2	99	2.01	5.6	<50	1.57		<100	2.91	1.80	0.66	0.26	1.02	<5000
23	GRA 98006,12	A/B	612	MWG	0.403	6.93	12.20	49.94	9.85	0.49	18.28	32.6	3.9	62	2.37	5.9	<40	1.6	75	38	2.42	1.53	0.61	0.26	1.06	<2300
	GRA 98033,11	A/B	581	MWG	0.438	6.98	11.25	50.41	9.80	0.55	19.48	33.7	3.1	54	2.09	7.9	<6	<3	74	38	2.93	1.81	0.71	0.31	1.16	<800
24	QUE 99005,6-A	B	302	MWG	0.378	6.59	12.46	49.29	9.96	0.54	18.94	31.1	4.1	55	2.15	3.79	<12	2.2	64	31	3.03	1.84	0.66	0.26	1.23	<1900
	QUE 99005,6-B		405	MWG	0.388	6.44	12.70	49.83	10.02	0.57	18.78	31.9	4.4	60	2.15	3.85	<13	2.1	77	<60	3.01	1.81	0.74	0.28	1.30	<1500
25	QUE 99006,7	B	506	MWG	0.45	6.51	12.45	50.28	10.25	0.50	18.35	33.0	4.4	63	2.08	6.5	<20	1.5[c]	67	30	2.50	1.40	0.65	0.26	1.52	<2000
Mg-rich (EET 87520) and cumulate (2–9) eucrites																										
1	EET 87520,10-A	B	327	MWG	0.47	6.44	13.44	50.58	11.00	0.50	16.47	29.7	3.4	75	2.34	4.0	0.10[c]	1.53	90	40	4.29	2.30	0.66	0.25	1.52	3.8
	EET 87520,10-B		328	MWG	0.47	6.99	13.98	49.80	9.78	0.61	17.41	27.4	3.4	76	2.67	4.5	<30	1.52	86	26	2.21	1.19	0.66	0.24	0.54	<2100
2	ALH 85001,25-a	A/B	330	MWG	0.270	12.93	13.71	50.20	8.94	0.42	12.45	17.6	1.9	103	5.0	15.5	<30	1.09	66	<40	0.77	0.54	0.42	0.09	0.38	<3000
	ALH 85001,25-b		330	MWG	0.291	12.87	13.70	50.20	8.88	0.43	12.44	17.3	2.0	103	5.0	13.9	2.9	0.63	59	<40	0.82	0.54	0.43	0.084	0.37	2.2
3	A-881819		320	NIPR	0.334	9.21	15.03	48.62	10.41	0.48	14.45	22.1	1.2	79	2.79	6.1	9	1.8	70	<20	0.61	0.39	0.43	0.073	0.30	<1300
4	A-881394,56-A		273	NIPR	0.085	8.56	14.97	52.38	10.87	0.38	11.75	20.6	0.9	82	2.62	7.8	7.7	0.93	67	<32	0.40	0.29	0.27	0.061	0.215	4.2
	A-881394,56-B		271	NIPR	0.092	8.61	14.21	51.67	10.93	0.40	12.45	24.7	1.1	78	3.77	7.1	<30	0.85	65	<35	0.40	0.32	0.30	0.06	0.23	<1800
5	EET 87548,7-A	B/C	341	MWG	0.179	13.44	5.86	49.54	6.88	0.66	21.01	31.0	1.3	109	7.6	12.1	<26	0.70	<35	<23	0.17	0.14	0.20	0.06	<0.11	<2600

	EET 87548,7-B		344	MWG	0.160	13.96	6.08	49.68	6.53	0.68	21.07	31.3	1.3	141	8.0	11.5	3.4	0.5[c]	<43	<15	0.20	0.14	0.18	0.06	<0.1	3.2
6	PCA 91159,5	B	378	MWG	0.318	11.19	10.16	49.15	8.47	0.54	18.88	28.4	2.4	105	4.82	12.9	0.46	0.89	62	30	1.14	0.81	0.47	0.15	0.56	1.5
7	Talampaya-A	fall	316	UCLA	0.201	12.84	12.40	50.34	8.42	0.47	14.50	19.5	0.27	85	3.43	11.6	<10	0.52	<60	<50	0.122	0.065	0.25	0.027	0.009[c]	<3000
	Talampaya-B		323	UCLA	0.229	13.22	11.91	49.16	8.08	0.49	15.37	20.4	0.56	88	4.39	16.6	<30	1.07	50	<60	0.105	0.070	0.29	0.025	0.092	<2000
8	Y-791195,73-A	A	235	NIPR	0.373	7.42	13.61	51.02	10.11	0.54	16.04	29.0	1.3	72	2.15	6.0	1.21	<3	66	<20	0.50	0.35	0.45	0.083	0.24	4.7
	Y-791195,73-B		244	NIPR	0.389	7.59	13.10	50.36	10.16	0.56	16.86	31.0	1.7	69	2.20	6.7	<30	1.11	75	<30	0.56	0.39	0.45	0.088	0.26	<3000
9	Y-791438,54		300	NIPR	0.200	11.28	13.06	50.04	9.41	0.52	14.17	21.6	1.3	82	2.52	7.2	0.95	0.88		<40	0.70	0.44	0.40	0.08	0.31	4.8
Diogenites (monomict, except Y-791200)																										
1	ALH 77256,96-a	A/B	381	MWG	0.009	28.2	1.53		1.62	0.49	18.81	21.9	0.7	162	8.6	36.1	35	0.44	<50	<40	0.12	0.099	0.008	0.05	0.08	79
	ALH 77256,96-b		369	MWG	0.009	24.9	1.65		1.45	0.52	16.54	19.4		149	7.6	33.1	29		<60	<40	0.15	0.084	0.010	0.043	<0.2	<1700
2	LAP 91900,26	A/B	561	MWG	0.011	25.4	0.56	55.57	1.12	0.49	15.60	14.1	0.4	104	5.3	13.9	18[c]	<2	<80	<150	<0.13	0.018	<0.1	0.013	<0.2	55
3	NWA 1461-A		445	Gregory	0.012	31.4	0.65	54.89	2.46	0.31	9.66	5.5	0.27	74	4.59	24.6	139	<0.4	<14	9.4	0.36	0.10	0.024	0.009	0.059	400
	NWA 1461-B		571	Gregory	0.007	30.4	0.66	56.46	0.97	0.31	9.87	5.6	0.23	72	4.79	26.7	155	<0.2	<12	6.0	0.07	0.053	0.011	0.009	0.032	<500
4	NWA 4283		465	Thompson	0.005	26.5	0.65	52.03	0.75	0.54	17.21	13.2	0.43	332	16.0	30.5	5[c]	<0.2	<18	<16	0.05	0.013	0.006	<0.006	<0.04	<1000
5	Y-75032,90	A	506	NIPR	0.084	21.7	2.79	51.34	3.60	0.57	19.50	24.9	1.8	117	5.0	17.5	27	0.38[c]	<50	<40	0.41	0.34	0.13	0.11	0.26	19
6	Y-791200,86		273	NIPR	0.193	17.6	6.0	51.24	5.28	0.56	17.90	22.6	1.8		4.51	13.9	15[c]	0.54	<50	<50	1.14	0.56	0.25	0.111	0.37	36
Relative uncertainty[b]					2	4	4	3	4	3	4	3	7	7	3	3	8	8	9	9	4	4	4	5	5	8

[a] In sample names, an ending of -A or -B designates analysis of separate chips; an ending of -a or -b designates replicate analyses of aliquots from a single powder.

[b] Normal uncertainty limits (% relative) for 70% confidence. Sampling errors sometimes predominate, however.

[c] Uncertainty greater than 30% relative; for a more complete itemization of uncertainties, see the Electronic Annex.

yses. In a few cases, mostly involving small chips such as Y-82202,63 (51 mg) and LEW 87295,8 (97 mg), the powdering step was deferred until after INAA. For two meteorites, manifest in Table 1 by absence of SiO_2 data, the chips were never powdered and consequently no MFBA was obtained.

In cases where we obtained two analyses from a single parent chip, we usually broke the chip into two subequal masses before powdering. But in some cases, designated by the use of a lower-case -a and -b at the end of the sample name in Tables 1–3, the two analyses were obtained from aliquots of a single powder. Note, however, that "Melrose (b)" is simply the name of this howardite; the "(b)" does not signify anything about our procedure in processing this sample. The sample mass listed in Table 1, 2 or 3 is the sum of the INAA mass and (if applicable) the fused-bead mass.

The main mass of each sample went for instrumental neutron activation analysis (INAA). Our INAA procedure was described by Kallemeyn (1993). Irradiations are obtained at the UC-Irvine reactor facility. INAA typically begins with a 60 s "rabbit" irradiation, followed by a single 200 s count to determine short-lived species: Mg, Al, Ti, V, Mn and Ca. Absence of V in an analysis (Tables 1–3) indicates that no rabbit irradiation was performed; and any Mg, Al or Ti data were derived exclusively by MFBA. Other elements (and replicate data for Mn and Ca) are determined after a subsequent 3–4 h irradiation, through a series of 4–5 separate, increasingly long counts that finally end about two months after the irradiation. Data analysis is based on the program SPECTRA (Grossman and Baedecker, 1986), which achieves optimal precision through the use of graphic display and interactive analysis of the γ-ray spectra. Integrations of the areas of small γ-ray peaks and multiplets are checked visually, and baseline parameters are adjusted where necessary. Where useful, upper limits were calculated for 99% (2.6 σ) confidence, based on counting statistics. In some cases, the same samples used for INAA were subsequently utilized for its radiochemical variant, RNAA. Samples analyzed by RNAA are distinguishable by inclusion of results for Ge, Re and Os in Tables EA-1–EA-3. As described by Warren et al. (1999), our RNAA procedure also provides more sensitive determination of Ni, Zn, Ir and Au; and in a few cases we applied it to determine Cd. Note that in the case of Ir, for which we determined concentrations ranging from 0.42 pg/g (in EET 87542, Table 1) to 59 ng/g (in LEW 85313,32-b, Table 3), we employ units of pg/g Table 1, but ng/g in Tables 2 and 3.

Sample names are abbreviated throughout the paper. The abbreviations in Tables 1–3 are the standard forms used in the Meteoritical Bulletin: A for Asuka, ALH for Allan Hills, CRE for Mount Crean, DaG for Dar al Gani, EET for Elephant Moraine, FRO for Frontier Mountain, GRA for Graves Nunataks, GRO for Grosvenor Mountains, HaH for Hammadah al Hamra, LAP for LaPaz Ice Field, LEW for Lewis Cliffs, MAC for MacAlpine Hills, MET for Meteorite Hills, NWA for Northwest Africa, PCA for Pecora Escarpment, QUE for Queen Alexandra Range, RKP for Reckling Peak, TIL for Thiel Mountains and Y for Yamato. For labeling points on figures, we use

Table 2
Bulk-rock compositional results for 22 elements in 31 polymict eucrites. For additional elements and itemization of uncertainties, see the Electronic Annex.

	Sample[a]	Weathering	Mass	Source	Na_2O	MgO	Al_2O_3	SiO_2	CaO	MnO	FeO	Sc (μg/g)	Ti (mg/g)	V (μg/g)	Cr (mg/g)	Co (μg/g)	Ni (μg/g)	Ga (μg/g)	Sr (μg/g)	Ba (μg/g)	La (μg/g)	Sm (μg/g)	Eu (μg/g)	Lu (μg/g)	Hf (μg/g)	Ir (ng/g)
1	ALH 78132,99	A	337	MWG	0.47	7.24	13.41	50.07	9.67	0.47	16.75	27.6	3.7	64	2.48	5.3	14[c]	<5	90	<80	2.71	1.82	0.64	0.27	1.00	<3
	ALH 78132,102		375	MWG	0.42	9.67	11.91	51.00	8.42	0.55	17.89	26.8	3.4	78	2.95	6.6	16[c]	<1.0	54	<80	3.04	1.50	0.55	0.24	1.19	0.87
2	A-9029		221	NIPR	0.32	12.28	10.53	49.09	8.21	0.52	17.22	24.7	3.5	94	4.47	11.4	38	1.4	65	<70	2.06	1.32	0.51	0.21	1.61	<2.3
3	Bialystok	fall	329	NM Wien	0.28	10.91	10.71	49.06	8.60	0.50	17.49	24.7	2.4	106	5.6	7.6	22	0.95	53	15[c]	1.34	0.894	0.39	0.155	0.63	30[d]
4	Dar al Gani 391		421	MPI Mainz	0.41	9.93	10.44	49.60	8.88	0.52	18.34	26.7	3.3	73	2.92	8.15	33	<1.1	58	30	3.5	1.96	0.56	0.25	1.31	<1.4
	Dar al Gani 411	W0	197	MPI Mainz	0.43	10.75	11.25	50.37	8.81	0.54	17.27	28.1	4.0	93	3.81	10.7	30	1.07	50	55	3.5	1.98	0.64	0.27	1.37	1.9
5	EET 79005,93	A	310	MWG	0.20	9.50	11.59	51.42	9.16	0.53	15.71	27.1	3.6		2.54	8.6	23	1.7	70	60	2.87	1.78	0.61	0.26	1.20	0.60
	EET 79005,95		305	MWG	0.37	10.69	10.67	49.49	9.53	0.53	17.01	24.9	3.6		2.78	5.9	11.6	<1.8	68	31	3.5	2.04	0.53	0.23	1.15	0.57
6	EET 82600,2-A	Ae	534	MWG	0.35	11.12	9.50	50.87	8.15	0.49	17.51	24.6	3.4	69	3.06	6.2	7.5[c]	<2	74	26[c]	2.37	1.11	0.52	0.193	1.12	<2
	EET 82600,2-B		526	MWG	0.41	10.07	11.07	49.70	9.19	0.49	17.12	25.2	3.3	64	2.81	5.5	10.2	<2	71	30	2.46	1.37	0.59	0.21	1.08	<2
	EET 82600,7		605	MWG	0.31	13.24	9.12	49.89	7.09	0.51	18.57	24.8	2.8	74	3.47	8.0	22	1.1	57	20	1.80	1.03	0.46	0.18	0.97	1.8
7	EET 92023,9-a	A	316	MWG	0.40	10.00	11.39	49.13	9.08	0.54	18.64	28.0	2.5	78	2.32	67	1350	1.40	76	<40	0.97	0.81	0.47	0.17	0.51	51
	EET 92023,9-b		313	MWG	0.38	10.0	11.4	49.13	9.06	0.53	18.31	24.9	2.4		2.11	59	1110	1.20		36	1.00	0.76	0.47	0.16	0.51	45
8	FRO 97045,23		461	EUROMET	0.39	8.37	12.18	48.88	9.62	0.52	18.41	25.1	3.0	76	2.69	6.7	10.5	0.97	59	25	2.41	1.00	0.57	0.204	1.26	<1.4
9	Igdi-A		479	ENS Lyon	0.44	5.43	11.74	48.78	11.35	0.51	19.98	32.8	5.4	61	1.74	8.7	59	2.4	95	107	4.1	2.41	0.74	0.36	1.87	2.2
	Igdi-B		244	ENS Lyon	0.43	5.47	11.21	48.46	11.92	0.53	20.27	32.1	5.1	51	1.72	5.6	31	<5	81	77	3.81	2.25	0.68	0.33	1.44	2.4
10	LEW 85303,90	A/B	306	MWG	0.43	7.37	11.80	49.21	9.97	0.55	18.87	31.8	3.3	62	2.31	12.0	78	<2	62	28	2.46	1.49	0.58	0.24	1.14	3.55
	LEW 85303,94		297	MWG	0.45	7.34	12.00	48.93	9.73	0.55	19.29	30.4	3.6	60	2.19	12.7	145	<1.6	65	60	3.8	2.03	0.65	0.33	1.36	11.2
11	LEW 87004,14	A	337	MWG	0.43	9.10	11.75	50.05	9.34	0.55	17.50	27.6	3.9		2.65	8.0	34	<1.2	74	27	3.03	1.9	0.56	0.26	1.19	1.21
	LEW 87004,19		328	MWG	0.47	8.05	12.35	50.12	9.75	0.55	17.12	28.0	4.9	74	2.54	9.4	41	<2.4	71	31	3.93	2.14	0.64	0.29	1.34	1.86
12	LEW 87026,7	A	305	MWG	0.40	8.99	11.29	49.95	8.94	0.53	18.24	28.1	3.8	83	3.14	5.8	26	1.11	70	23	2.13	1.08	0.61	0.22	1.19	2.00
13	LEW 87295,7	B	283	MWG	0.41	9.34	11.26	50.10	9.06	0.56	18.13	27.4	3.3		2.64	10.2	97	<1.2	63	38	2.61	1.47	0.52	0.22	1.00	12.0
	LEW 87295,8		97	MWG	0.39	11.79	8.88	48.67	7.19	0.66	21.42	27.1	2.4	99	3.94	16.9	226	1.1	<60	<50	2.25	1.27	0.45	0.181	0.67	9.0
14	LEW 88005,19	B	655	MWG	0.43	6.75	13.36	49.58	10.18	0.50	18.27	28.4	3.7	56	2.02	4.49	<30	<2	71	32	1.81	0.97	0.50	0.20	0.95	<3
15	Macibini	fall	382	AMNH	0.45	8.38	11.90	49.73	9.50	0.53	17.71	27.4	4.7	72	2.97	8.4	24	<3	60	<45	3.0	1.89	0.66	0.28	1.34	1.10
16	PCA 82502,85	A	218	MWG	0.40	6.64	13.02	48.83	10.24	0.54	18.91	31.9	4.1	60	2.13	5.6	<30	1.12	90	33	1.75	1.47	0.68	0.22	1.46	<3.7
	PCA 82502,86		224	MWG	0.40	6.66	12.76	49.67	10.14	0.54	18.63	31.8	4.4	68	2.09	5.9	18	1.53	73	38	0.99	0.83	0.66	0.21	1.43	<2.6
17	PCA 91007,4	A/Be	328	MWG	0.46	6.00	13.0	49.92	10.34	0.53	18.16	30.6	4.4	68	2.03	6.0	7.5	1.3[c]	94	<33	3.0	2.16	0.68	0.32	1.44	0.26
18	QUE 97004,7	A	309	MWG	0.44	6.73	12.5	49.03	10.14	0.56	19.17	29.6	3.9	60	2.13	91	195	<3	81	37	2.57	1.63	0.60	0.23	1.20	7.1
19	TIL 82403,30	A	310	KOPRI	0.47	7.00	12.2	48.89	10.35	0.55	18.68	30.6	4.4	70	2.73	4.94	14[c]	<1.3	<70	<120	4.3	1.78	0.61	0.238	1.62	<2.8
	TIL 82403,31		404	KOPRI	0.51	6.88	13.3	49.29	10.26	0.54	18.64	31.8	4.3	69	2.28	5.9	7.7	1.42	91	<70	1.06	0.82	0.73	0.21	1.37	0.64
20	Y-74159,79-a	A	349	NIPR	0.47	8.12	11.95	50.97	9.38	0.54	17.48	29.4	4.7	65	2.62	4.91	16[c]	<1.5	80	62	4.9	2.34	0.69	0.34	1.60	<3
	Y-74159,79-b		349	NIPR	0.46	7.97	11.99	50.97	9.35	0.52	17.47	29.2	4.8	64	2.60	5.5	8[c]	<1.5	80[c]	<74	5.0	2.30	0.69	0.33	1.68	<2.2
21	Y-74450,111	A	543	NIPR	0.52	7.47	12.01	49.45	9.90	0.49	18.63	30.3	5.1	61	2.69	11.2	22	1.6	<80	<50	4.7	2.72	0.72	0.37	1.82	2.3[c]
22	Y-75015,88	A	535	NIPR	0.43	7.21	11.83	49.55	10.05	0.46	18.74	29.9	6.0	69	3.42	8.9	<25	1.21	<90	<60	3.8	2.29	0.67	0.33	1.55	<3.5
23	Y-790007,84	A	526	NIPR	0.47	7.55	11.89	49.33	9.92	0.48	18.64	29.8	5.0	59	2.64	8.0	<50	1.11	<90	<60	4.7	2.72	0.72	0.37	1.80	<3
24	Y-790260,91	A	521	NIPR	0.45	7.5	12.3	49.81	9.25	0.50	18.21	29.5	4.8	70	2.36	6.9	11.9	0.69	80	<35	4.1	2.06	0.64	0.33	1.81	<1.3
25	Y-790266,102	A	523	NIPR	0.51	7.17	12.74	49.41	9.78	0.51	18.46	29.3	5.2	77	2.57	6.8	9.7	<2	52	42[c]	4.6	2.72	0.70	0.35	1.70	0.43
26	Y-791192,81-a		331	NIPR	0.29	12.93	10.40	50.34	7.52	0.50	16.40	21.8	2.0	95	4.87	11.7	6.1	<1.3	34	<60	0.90	0.50	0.40	0.119	0.34	<1.1
	Y-791192,81-b		333	NIPR	0.26	13.18	10.57	50.34	7.64	0.52	16.40	21.1	2.6	107	4.83	11.3	4.6	0.90		<30	0.81	0.53	0.43	0.126	0.41	0.028
27	Y-791826,57-A		345	NIPR	0.52	7.54	11.46	49.57	9.78	0.50	18.54	28.9	6.2	61	2.53	6.4	14[c]	<2.5	<300	<200	4.7	2.77	0.73	0.37	1.75	<2.5
	Y-791826,57-B		347	NIPR	0.51	7.87	11.47	49.21	9.80	0.52	19.06	29.8	4.9	67	2.59	10.3	8[c]	<5	78	56	4.1	2.51	0.71	0.35	1.61	2.0[c]
28	Y-793164,68-a		317	NIPR	0.55	5.61	12.25	49.44	10.12	0.55	19.52	33.6	5.5	57	1.99	5.4	<8	1.33	60	<30	3.2	1.78	0.72	0.31	1.82	<1.5
	Y-793164,68-b		314	NIPR	0.55	5.74	12.23	49.44	10.13	0.55	19.53	33.7	5.5	57	2.00	5.3	9.3	1.7[c]	66	<30	3.1	1.78	0.72	0.33	1.85	<1.6
29	Y-794002,60-A		351	NIPR	0.51	7.61	12.06	49.42	10.06	0.45	17.74	26.9	5.4	52	2.62	7.1	<20	<2	<90	<90	4.2	2.51	0.70	0.33	1.69	<3
	Y-794002,60-B		340	NIPR	0.49	8.29	11.68	49.17	9.59	0.49	18.23	26.2	4.9	62	2.56	5.5	<30	2.46	<140	<70	4.2	2.50	0.67	0.32	1.61	<3
30	Y-82052,63		567	NIPR	0.40	10.33	11.14	50.29	8.65	0.51	16.99	25.0	3.8		4.02	9.2	29	1.2[c]	48	25	2.54	1.53	0.49	0.21	1.02	1.19
31	Y-981651,65		250	NIPR	0.40	10.05	11.99	49.47	9.34	0.51	16.84	26.0	2.9	68	3.21	10.5	<25	0.8[c]	60	38	1.34	0.91	0.57	0.19	0.61	<2.7
Relative uncertainty[b]					2	4	4	3	4	3	4	3	7	7	3	3	8	8	9	9	4	4	4	5	5	8

[a] In sample names, an ending of -A or -B designates analysis of separate chips; an ending of -a or -b designates replicate analyses of aliquots from a single powder.

[b] Normal uncertainty limits (% relative) for 70% confidence. Sampling errors sometimes predominate, however.

[c] Uncertainty greater than 30% relative; for a more complete itemization of uncertainties, see the Electronic Annex.

[d] Bialystok results are anomalously high for Ir and especially Au (Table EA-2) ; we suspect artificial contamination.

Table 3
Bulk-rock compositional results for 22 elements in 31 howardites. For additional elements and itemization of uncertainties, see the Electronic Annex.

	Sample[a] weathering		Mass	Source	Na_2O	MgO	Al_2O_3	SiO_2	CaO	MnO	FeO	Sc (μg/g)	Ti (mg/g)	V (μg/g)	Cr (mg/g)	Co (μg/g)	Ni (μg/g)	Ga (μg/g)	Sr (μg/g)	Ba (μg/g)	La (μg/g)	Sm (μg/g)	Eu (μg/g)	Lu (μg/g)	Hf (μg/g)	Ir (ng/g)
1	Chaves-a	fall	327	J. Monteiro	0.224	19.01	6.45	52.51	5.23	0.48	14.68	18.6	2.4	81	3.79	16.7	65	0.41[c]	44	24	1.59	0.93	0.33	0.138	0.68	1.07
	Chaves-b		303	J. Monteiro	0.233	19.20	6.46	52.51	5.24	0.48	14.77	19.1	1.9	88	4.08	19.5	67	0.61	29	<40	1.66	0.99	0.33	0.134	0.60	<3
	Chaves-c		294	J. Monteiro	0.241	19.15	6.58	52.51	5.24	0.49	14.73	18.7	2.2	93	4.09	16.5	53	0.71[c]	<60	19	1.62	0.96	0.32	0.145	0.69	<3
2	CRE 01400,10	B	569	MWG	0.257	16.45	7.19	51.12	5.87	0.49	16.90	21.4	2.5	101	5.1	17.9	37	<2	33	20[c]	2.31	1.18	0.33	0.157	0.64	1.70
3	Dar al Gani 779	W1	602	U. Freiburg	0.27	18.14	5.36	51.72	5.49	0.46	16.29	19.0	1.8	109	6.1	22.4	84	<1.2	52	320	1.20	0.63	0.24	0.108	0.51	2.81
4	EET 96003,8	A	312	MWG	0.28	13.30	10.72	49.80	8.04	0.51	16.10	22.0	2.0	93	4.09	12.8	15	0.77	49	32	1.32	0.81	0.37	0.126	0.56	0.9[c]
5	EET 99408,7	A/B	568	MWG	0.36	10.33	11.45	49.64	8.47	0.49	17.31	25.1	3.3	73	2.78	11.2	30	<1	48	30	2.97	1.87	0.57	0.25	1.01	1.78
6	GRO 95574,7	A	426	MWG	0.225	15.48	8.30	50.52	6.45	0.50	16.72	21.1	2.2	110	4.87	23.7	118	<0.8	<40	16	1.37	0.86	0.33	0.138	0.63	5.3
7	GRO 95581,8	A	562	MWG	0.256	15.52	7.68	49.96	6.39	0.52	17.43	23.0	2.6	99	5.2	19.8	153	<2	39	<30	1.58	0.97	0.39	0.165	0.75	5.3
8	HaH 285[d]	W2	307	U. Munster	0.171	18.12	5.28	49.96	7.08	0.49	16.55	17.1	1.6	116	5.4	18.2	63	<7	95	280	2.01	0.84	0.27	0.116	0.50	2.4
9	Hughes 004-A	?? (shiny	347	AMNH	0.258	13.92	8.66	49.97	7.15	0.53	17.85	24.2	2.7	100	4.50	11.3	12	0.60	47	23	1.59	0.99	0.38	0.148	0.69	<2
	Hughes 004-B	crust)	186	MPI Mainz	0.217	14.08	9.70	48.80	7.45	0.52	17.17	21.3	1.5	124	7.1	10.9	<15	0.61	43	22	1.62	0.91	0.42	0.120	0.37	<2
10	Jodzie	fall	484	Field M.	0.31	13.53	8.99	50.42	7.11	0.49	17.46	24.6	2.2	83	4.12	50.1	840	1.7	<50	35	1.68	0.99	0.47	0.16	0.93	38.4
11	LEW 85313,32-a	B	373	MWG	0.30	14.67	7.91	49.97	6.56	0.48	18.03	21.0	1.8	78	4.10	57	1130	<1.4	<80	37	1.34	0.83	0.31	0.135	0.60	50
	LEW 85313,32-b		378	MWG	0.29	14.90	8.22	49.97	6.63	0.49	18.02	20.6	2.5	93	4.02	66	1110	<4	<150	<40	1.32	0.83	0.32	0.125	0.54	59
12	LEW 87002,7	Ae	240	MWG	0.104	20.40	5.32	51.07	4.36	0.54	16.87	16.9	2.0	91	4.37	13.1	14.2	0.63	<70	<30	2.65	1.31	0.28	0.156	0.62	0.39
13	LEW 87005,8	A	376	MWG	0.38	9.22	11.35	48.81	9.06	0.51	18.64	26.9	3.5	72	2.72	16.0	218	0.72[c]	63	37	2.20	1.46	0.52	0.21	1.03	14.2
14	MAC 02666,9	B	496	MWG	0.42	9.29	11.50	49.21	9.14	0.53	18.51	27.4	3.6	73	2.86	28.1	330	<2	50	36	2.50	1.50	0.53	0.23	1.01	11.0
14	Mässing	fall	373	Humbolldt U.	0.251	17.48	6.36	51.18	5.58	0.54	17.34	22.1	2.5	93	4.73	14.7	61	0.8	35	24[c]	1.72	1.08	0.36	0.172	0.80	1.69
16	Melrose (b)		232	MPI Mainz	0.161	15.13	8.00	49.84	5.40	0.56	18.80	25.1	3.0	128	7.5	10.5	38	3.7[c]	29	66	3.2	1.18	0.37	0.187	1.08	2.3
17	MET 00423,5	A/B	534	MWG	0.35	12.04	10.29	49.95	8.17	0.52	18.05	25.7	2.7	90	3.66	20.0	228	<2	60	37	1.99	1.18	0.46	0.187	0.78	7.0
18	MET 01087,6	B	363	MWG	0.241	17.07	7.42	48.73	5.74	0.49	18.63	19.9	2.3	96	5.3	18.7	145	<1.2	42	<30	0.67	0.57	0.33	0.128	0.70	4.3
19	MET 96500,11	B	540	MWG	0.30	10.15	10.24	49.01	10.67	0.46	17.15	24.4	3.1	66	2.91	9.8	55	0.74	51	<30	1.43	1.29	0.47	0.163	0.92	6.3
	MET 96500,12		594	MWG	0.32	13.33	8.80	49.83	7.13	0.50	18.41	26.3	2.9	75	3.58	38.2	450	<1.4	62	36	3.3	2.01	0.49	0.26	1.09	4.3
20	Muckera 002		171	MPI Mainz	0.36	10.72	9.63	49.25	9.21	0.55	19.45	27.6	4.5	77	3.55	18.6	170	<1.3	71	90	5.2	2.83	0.67	0.35	1.91	5.5
21	NWA 1182-A (light)		593	Lang	0.207	16.54	7.52	51.18	6.03	0.49	16.29	20.3	2.69	92	4.54	12.1	19	<2	<80	32	1.53	0.85	0.30	0.141	0.94	<3
	NWA 1182-B (dark)		248	Lang	0.30	13.49	9.52	50.15	7.50	0.53	17.41	23.7	2.79	102	3.97	33.7	450	<2	<80	46	1.80	1.06	0.43	0.168	0.87	18
22	NWA 1282		401	Hupe	0.39	9.94	11.24	50.08	8.84	0.52	17.82	27.9	3.7	71	3.11	12.3	76	1.1	<80	40	2.7	1.70	0.59	0.27	1.26	3.6
23	Pavlovka	fall	340	Field M.	0.214	17.44	6.51	51.33	5.40	0.54	17.26	23.5	2.1	126	7.0	23.9	144	0.20	49	19	1.15	0.71	0.32	0.12	0.50	5.7
24	PCA 02009,5[e]	A/B	408	MWG	0.028	26.68	1.22	51.78	1.32	0.47	17.02	12.3	1.0	89	4.63	23.3	109	<2	<60	<20	0.143	0.099	0.038	0.030	0.072	4.0
25	QUE 94200,21	A/B	514	MWG	0.185	18.66	5.72	51.44	4.67	0.49	16.76	18.8	2.2	108	5.5	35.0	148	<1.4	31	28	1.71	1.02	0.29	0.145	0.70	4.5
26	QUE 97001,8	A	493	MWG	0.265	16.50	7.32	51.95	5.72	0.49	15.84	20.4	2.6	91	4.87	14.1	44	<2	<70	<40	1.66	0.93	0.34	0.131	0.78	1.5
27	QUE 99033,11	A/B	630	MWG	0.197	18.18	5.75	52.27	4.73	0.46	16.53	19.9	1.9	99	5.5	17.6	33	<1.2	30	<30	1.20	0.85	0.27	0.137	0.70	1.00
28	Y-7308,108		312	NIPR	0.129	20.89	4.71	50.53	4.13	0.55	17.07	19.0	1.5	119	6.0	14.3	25	0.56	14[c]	<25	0.66	0.45	0.192	0.084	0.30	<1.1
29	Y-791573,83		460	NIPR	0.234	17.41	6.99	49.55	5.78	0.52	17.51	21.2	2.4	95	5.2	25.3	244	0.73	35	<45	1.44	0.90	0.34	0.150	0.62	9.9
30	Y-82049,65-A		354	NIPR	0.31	14.66	8.55	50.59	6.73	0.57	17.28	23.1	2.8		4.94	15.9	100	<1.5	55	<40	1.67	1.05	0.38	0.158	0.71	5.6
	Y-82049,65-B		325	NIPR	0.30	14.01	8.58	50.75	6.97	0.53	17.41	24.1	2.9	94	4.42	17.9	108	<1.8	46	21[c]	1.98	1.18	0.43	0.18	0.76	4.4
31	Zmenj	A/B	473	NM Wien	0.191	19.44	5.05	50.43	4.58	0.53	17.99	21.4	1.6	119	7.1	21.5	97	0.68	30	<40	0.92	0.66	0.27	0.119	0.48	3.0
Relative uncertainty[b]					2	4	4	3	4	3	4	3	7	7	3	3	8	8	9	9	4	4	4	5	5	8

[a] In sample names, an ending of -A or -B designates analysis of separate chips; an ending of -a, -b or -c designates replicate analyses of aliquots from a single powder.

[b] Normal uncertainty limits (% relative) for 70% confidence. Sampling errors sometimes predominate, however.

[c] Uncertainty greater than 30% relative; for a more complete itemization of uncertainties, see the Electronic Annex.

[d] Hammadah al Hamra 285.

[e] Although PCA 02009 as a whole is a howardite, the chip we analyzed is a polymict but nearly pure diogenite.

a four-character system. In the case of numerically named Antarctic and desert samples, the first letter of the standard abbreviation is combined with the last three integers of the numerical portion of the name (e.g., CRE 01400 abbrevi-

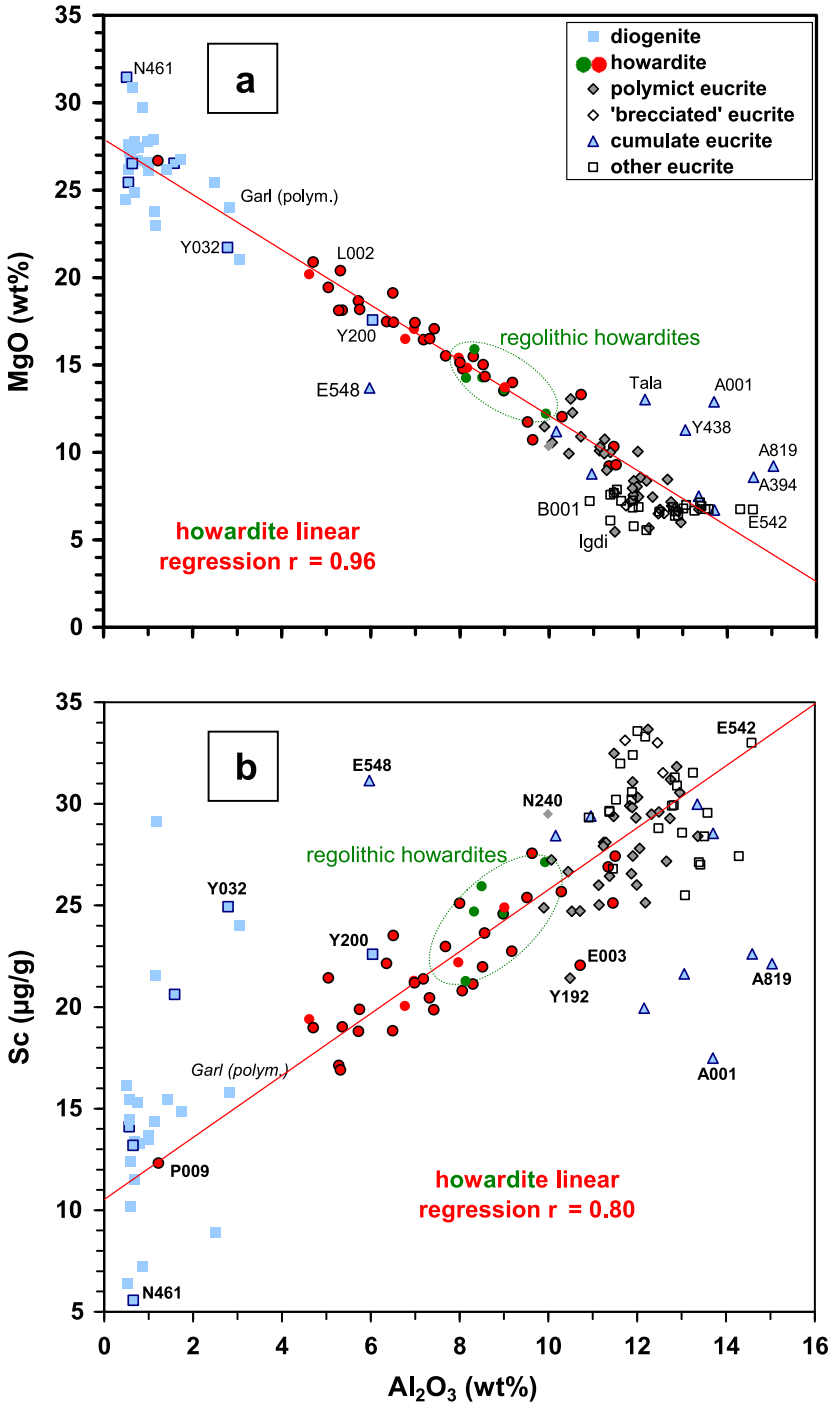

Fig. 1. The HED mixing trend: bulk-rock (a) Al_2O_3 vs. MgO and (b) Al_2O_3 vs. Sc. On this and other diagrams, symbols bounded by dark lines denote new analyses from this work (for each meteorite, the average of our 1–3 analyses is plotted). Included for completeness and shown by symbols without dark-line boundaries are averaged literature data for 10 well-studied howardites (Table EA-5) and the diogenites A-881377, A-881526 (assumed paired with A-881548 and A-881377), A-881839, Bilanga, Dhofar 700, EET 79002, EET 83246, Ellemeet, GRO 95555, Ibbenbüren, Johnstown, LEW 88008, Manegaon, MET 00422, MET 00424 (assumed paired with MET 00436), MET 00425, NWA 4272, PCA 91077, Roda, Shalka, Tatahouine and TIL 82410; and the polymict diogenite Garland. The diogenite literature references are too numerous to fully enumerate, but include Mittlefehldt (1994), Jochum et al. (1980), Yanai and Kojima (1995), Welten et al. (1997) and Barrat et al. (2008b). The regression lines are based on all howardites excepting our atypical sample of PCA 02009. For simplicity, we have here included in the cumulate category three eucrites that are arguably "Mg-rich" without being cumulates (see text). The "other eucrite" category comprises noncumulates that are either unbrecciated or monomict-brecciated.

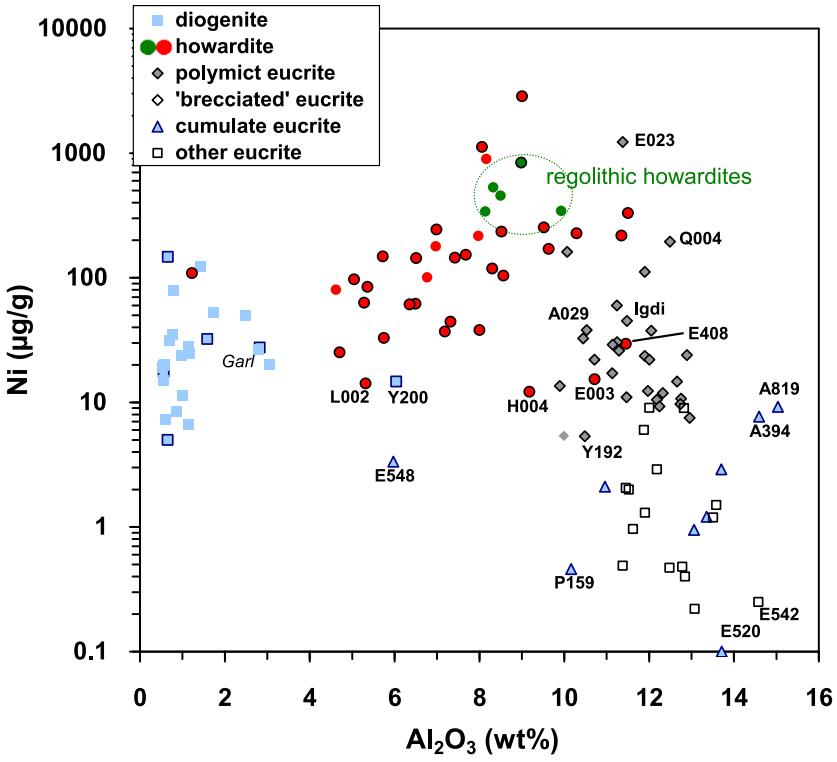

Fig. 2. A record of mixing between igneous HED materials and chondritic-impactor debris: bulk-rock Al_2O_3 vs. Ni. Regarding symbols and data sources cf. Fig. 1.

ates as C400). For all other samples, the abbreviation used in the figures is simply the first four letters of the name; e.g., Melrose (b) abbreviates as Melr. For plotting and discussion purposes, we assume the DaG 391 and 411 polymict eucrites are paired; and that the "brecciated" eucrites GRA 98006 and GRA 98033 are paired. A few other possible pairings are discussed in Section 3.2 (and its supplement in the Electronic Annex), as our new results help to constrain the pairing issue.

3. RESULTS

3.1. The basic two-component mixing trends

Results are shown in Tables 1–3; and in Tables EA-1–EA-4 of the paper's Electronic Annex. To zeroeth approximation the compositions (Fig. 1) are consistent with the hypothesis that howardites are basically two-component mixtures of eucrite + diogenite (Jerome, 1970; Jerome and Goles, 1971; McCarthy et al., 1972; Dreibus et al., 1977; Fukuoka et al., 1977), while polymict eucrites are pure or nearly pure eucrite (Delaney et al., 1984). All or virtually all of the polymict breccias also include a minor component of foreign chondritic matter that has importance for the bulk compositions only in terms of siderophile trace elements (Chou et al., 1976; Fig. 2). As noted as early as Mittlefehldt (1979), and discussed in detail below, this simple two-component mixing model for HED lithophile materials is oversimplified. Still, it provides a useful framework for discussion of the basic polymict-HED compositional trends. In the two-component mixing trends, the diogenite end member is richer by about a factor of four in MgO (Fig. 1a), a roughly similar factor for Co (which shows considerable scatter among diogenites), and a factor of ~2 for V (Fig. 3a). The eucrite end member is richer in most other elements, with the eucrite/diogenite concentration ratios especially high for Al_2O_3 (Fig. 1), CaO (Fig. 4), incompatible elements (Fig. 3b) and Sc (Fig. 4). On these diagrams, along with our new data, we include literature averages for up to 23 additional diogenites and 10 additional howardites (Table EA-5). The figures also include literature data for a few unusual eucrites: ALH 81001, Lakangaon and Nuevo Laredo (Warren and Jerde, 1987), the partial cumulate Pomozdino (Warren et al., 1990), and the impact-melt breccia NWA 1240 (Barrat et al., 2003).

3.2. Classification issues and outlier samples

As emphasized by Delaney et al. (1983, 1984) and Mason (1983), the HED polymict breccias are a mixing continuum. For descriptive purposes it is helpful to recognize howardites as a distinct medial class, but criteria for demarcation between howardite and polymict eucrite, and between howardite and polymict diogenite, are perforce arbitrary. Mason (1983) argued that the least arbitrary approach is to regard any HED containing any finite amount of diogenitic pyroxene along with eucritic matter as a howardite. However, Mason's approach seems impractical.

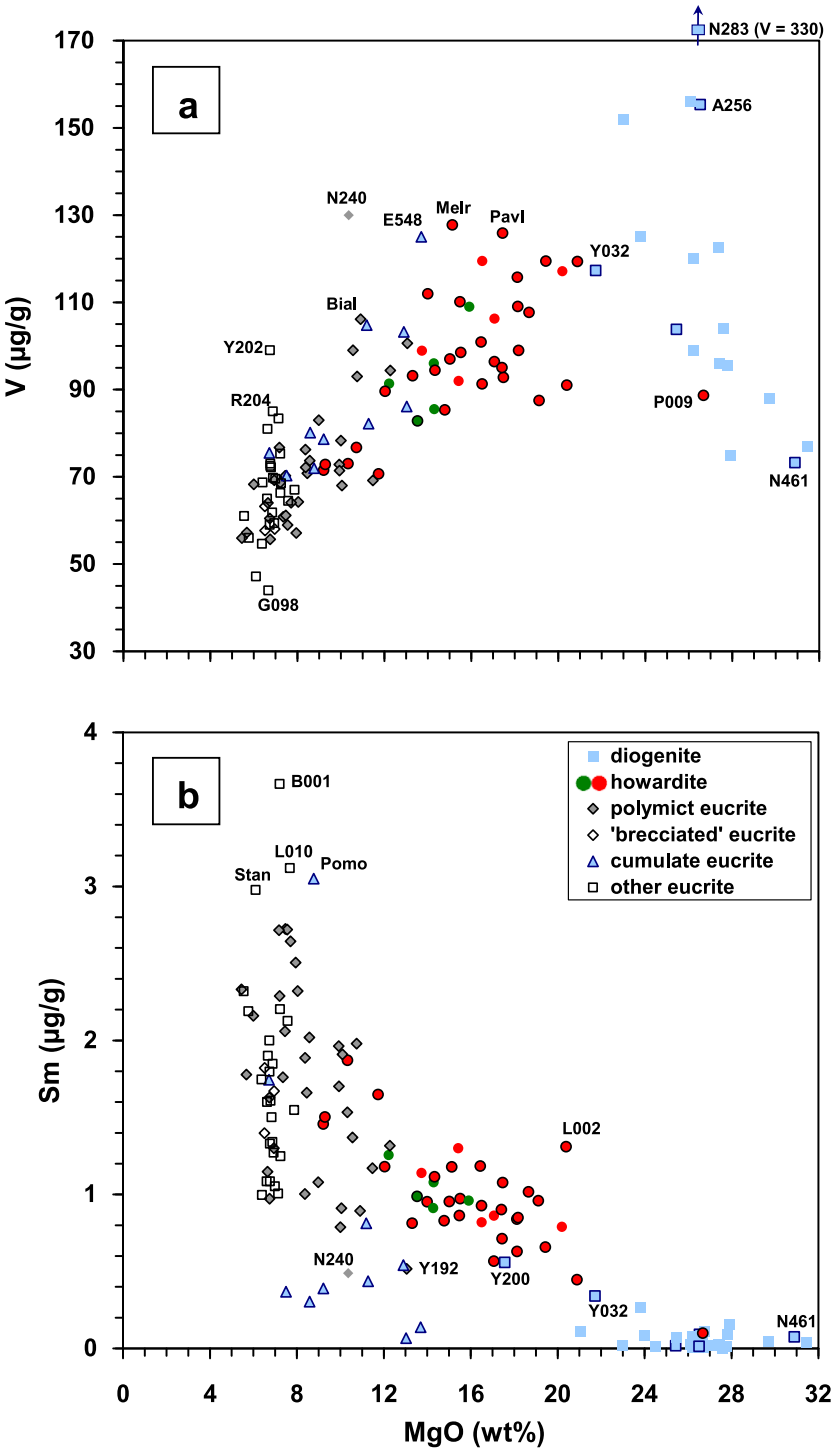

Fig. 3. More complex versions of the HED mixing trend: bulk-rock (a) MgO vs. V and (b) MgO vs. Sm. The howardite Muckera 002 has been excluded from the database for (b), because its REE have been enriched by desert weathering. In (a), much of the scatter among the diogenites and howardites is probably traceable to the spotty distribution of Cr-spinel, a major repository for diogenitic V at the scale (usually <<1 g) of our analyses. Regarding symbols and data sources cf. Fig. 1.

Detection of a mere trace of diogenite or eucrite (potentially of a magnesian cumulate variety) may be difficult. Furthermore, a classification-size bias may be introduced, because difficulty of trace component detection presumably varies as a function of sample size. A large meteorite yielding multiple large thin sections will more reliably manifest its trace component than a small meteorite sampled through one small thin section. For these reasons, we prefer the definition of howardite proposed by Delaney et al. (1984): an HED polymict breccia in which neither eucrite alone nor

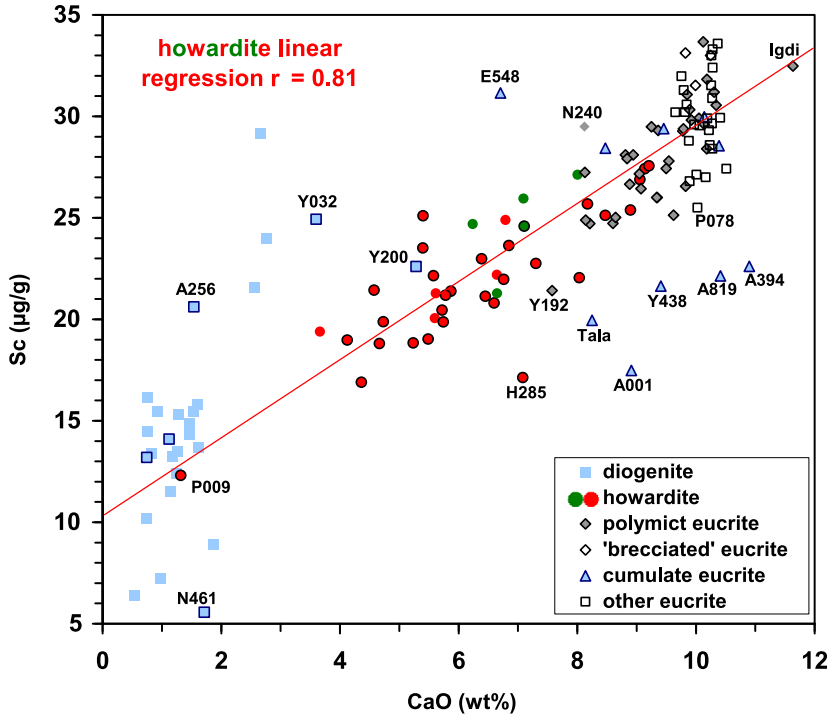

Fig. 4. The HED mixing trend: bulk-rock CaO vs. Sc. The regression line is based on all howardites excepting our atypical sample of PCA 02009 and the badly weathered HaH 285. Regarding symbols and data sources cf. Fig. 1.

diogenite alone constitutes over 90% by volume of the material. This definition still leaves classification of borderline cases prone to sampling problems, but the obvious arbitrariness of "90%" should at least have the advantage of reinforcing the notion that the HED polymict breccias are a mixing continuum, and discourage false apprehensions that, e.g., classification of a meteorite as a diogenite-poor howardite implies a clear genetic distinction from polymict eucrite. In any event, our philosophy in this work, mindful of the arbitrariness just discussed, has been to generally accept previous classifications (as compiled in the on-line Meteoritical Bulletin database maintained by J.N. Grossman), except in cases where our new observations clearly call for revision. We also propose recognition of regolithic howardite as a new, genetically significant subclass, but that issue will be discussed later in the paper.

In most cases, our new data are consistent with previous Meteoritical Bulletin classifications. Eleven of our samples were classified as "brecciated" eucrites, with no indication as to whether they are monomict or polymict. In some other cases, the new data imply an alternate, or more specific, classification. In most cases of generic "brecciated" classification, our siderophile results constrain the mixing issue. EET 87542, LEW 86002, LEW 87010, PCA 91159 and RKP 80204 all are extremely siderophile-depleted, and thus probably (as far as we have sampled them) monomict. QUE 97004 (which is a granoblastic breccia) and TIL 82403 are both siderophile-rich and manifestly polymict.

Newly classified here is the small (21 g), unusually Al_2O_3-rich howardite NWA 1282. Our analyzed chip had 11.2 wt% Al_2O_3 (Table 3). The fusion crust (average of 26 analyses) indicates, in wt%: MgO 10.62, Al_2O_3 10.16, SiO_2 50.16, CaO 8.41, TiO_2 0.65, FeO 18.44. A random sampling of 100 pyroxenes indicates that 24–28% of them are of diogenite origin (i.e., 24 have $En_{65–81}Wo_{1–4}$ composition; ~4 others are borderline-diogenitic). The rest encompass a wide variety of eucritic pyroxene compositions. A most distinctive feature is the presence of K-rich glassy spheroids (Fig. 5). Among four glassy spheroids in our thin section, K_2O ranges from 0.84–1.01 wt%; the spheroid compositions are otherwise nondescript polymict-HED (e.g., 8.1–13.4 wt% MgO, 9.4–12.4 wt% Al_2O_3). The only precedents for HEDs containing glassy spheroids this K_2O-rich are howardites NWA 1664 and NWA 1769 (Kurat et al., 2003; Barrat et al., 2008a). We suspect NWA 1282 may be paired with these other two distinctive NWA howardites.

Four of our samples are currently classified as "Mg-rich" but not cumulate eucrites. The monomict breccia PCA 91159 is also Mg-rich. Of these five, the unbrecciated EET 87548 and the monomict-brecciated ALH 85001 are clearly cumulate eucrites, because along with generally equant mineral grains they have incompatible element concentrations at levels too low to plausibly represent any plagioclase-saturated HED melt. The term "Mg-rich eucrite" is arguably appropriate for the unbrecciated and normally incompatible-element-rich EET 87520, which Mayne et al. (2009) classify as noncumulate. However, EET 87520 has also been interpreted as a cumulate (Carlson and Lugmair, 2000) or partial cumulate (Mittlefehldt and Lindstrom, 2003). PCA 91159 is analogous. Brecciation has obscured the original texture (surviving grains are up to 2.4 mm across), but it shows mineralogical affinity with cumulate eucrites (Bjonnes and Delaney, 2004), and has, to a mild

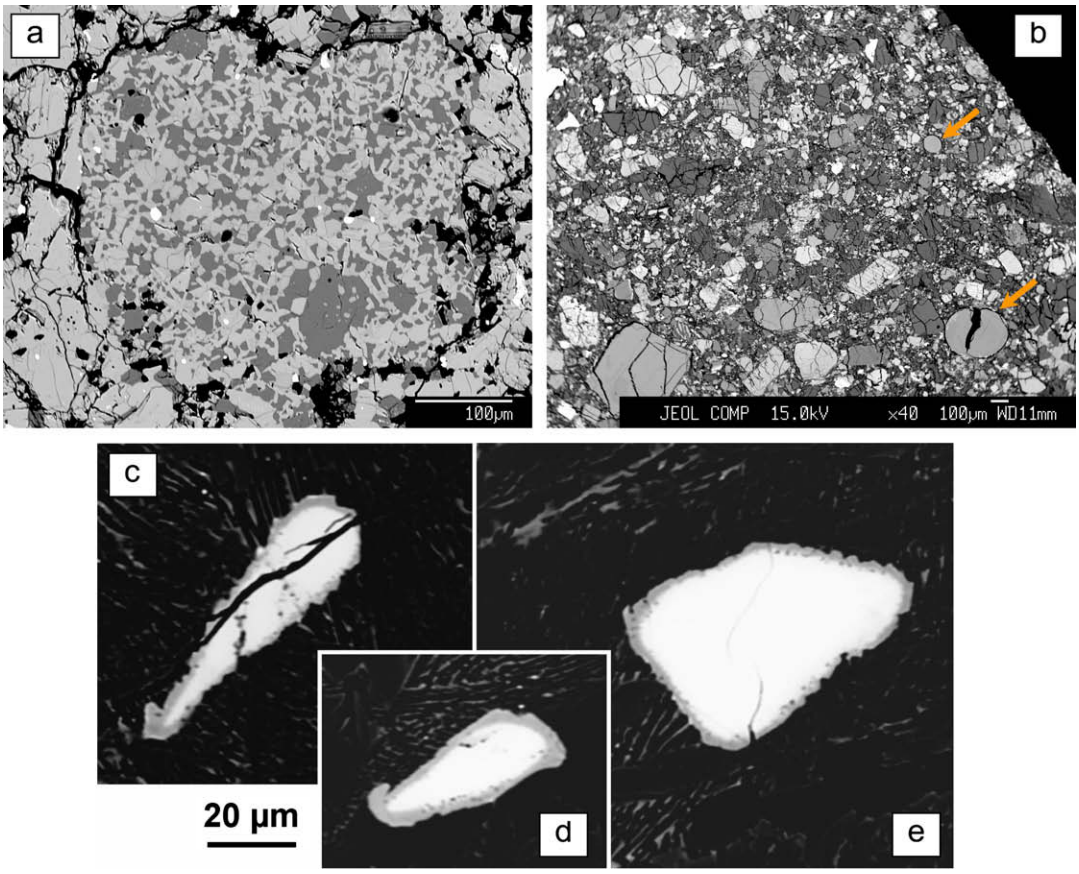

Fig. 5. Backscattered-electron images of (a) one of many incongruously fine-grained basaltic (impact-melt?) clasts in LEW 87002,5; (b) NWA 1282, showing (arrows) two of the four distinctively K-rich impact-melt spheroids in our thin section; (c), (d) and (e) Y-981651,50-1, showing scalloped, Cr- and Fe-poor corrosion rims (gray) on three Cr-spinels (white). Fine-grained groundmass around the Cr-spinels can be discerned (barely) from aligned clusters of elongate Fe-rich pyroxenes (gray). Scale bars in (a) and (b) denote 100 μm; in (c)–(e) 20 μm.

extent, cumulate-like low incompatible concentrations (Fig. 3b). For the sake of simplicity, these three "Mg-rich" eucrites are classified as cumulates in our Figs. 1–4 and 6. Our final "Mg-rich eucrite," breccia LEW 87002, is most difficult to classify; as discussed in the Electronic Annex of this paper, we regard it as a cumulate eucrite-rich howardite. Classification issues for numerous additional samples are also covered in the Electronic Annex.

3.3. Weathered samples

Samples of outlier composition are of interest as potential constraints on petrological diversity within the HED crust. But some scatter may be the result of weathering. Fourteen of our samples are finds from warm deserts, notorious sources of weathered meteorites. However, only DaG 779 (W1) and HaH 285 (W2) have been classified as showing visible indications of serious weathering. DaG 391/411 (paired) is W0. The 11 others, Agoult, Bluewing 001, Hughes 004, Igdi, Melrose (b), Millbillillie, Muckera 002, NWA 1182, NWA 1282, NWA 1461 and NWA 4283, have not been classified for weathering, although Barrat et al. (2003) noted evidence of weathering from high Sr, Ba and Pb concentrations in Igdi. We do not determine Pb, and our Sr and Ba data are generally not as precise as those of Barrat et al. (2003), but they can serve as checks for severe weathering. In terms of Ba, only DaG 779 and HaH 285 have obvious enrichments over normal HED levels. Muckera 002 and our "A" sample of Igdi also show enrichments marginally (given our modest precision for Ba) above normal HED levels. Our results for Sr are generally analogous, except DaG 779 is not much more than marginally enriched, and our Igdi "A" is slightly more obviously enriched (cf. Barrat et al., 2003). DaG 779, Melrose (b), HaH 285, Bluewing 001, and especially (and most mysteriously, since it is an Antarctic eucrite) FRO 97045 also appear U-enriched.

Bluewing 001 also shows obvious enrichment in Sr and especially in As (15 μg/g). However, Bluewing 001 has Ba in normal proportion to other incompatible elements, and normal La/Lu for its (extraordinarily high) overall REE enrichment level. Also, as shown by Warren and Gessler (2001), Ti zonation trends in its completely unequilibrated pyroxenes indicate that this material was extraordinarily incompatible-enriched on the parent asteroid (in the mineralogically simple HED system, Ti behaved as an incompatible element until end-stage conditions brought ilmenite onto the liquidus: e.g., BVSP, 1981; Warren and Jerde, 1987). Both Igdi "B" and Muckera 002 also show marginally suspect-high Sr.

The diogenite NWA 1461 also evinces weathering, by anomalously high La in relation to heavier rare-earth elements (REE; however, like most diogenites NWA 1461 is REE-poor; in absolute sense, the La enrichment is not great). A few of our samples also show clear Ce anomalies: negative anomalies in Melrose (b) and CRE 01400; positive in PCA 82502, MET 01087 and LEW 87026. In general, these few manifestly weathered samples do not figure prominently in our discussion (below) of the HED compositional trends; they merely augment the overall trends. The few exceptions will be noted as we come to them.

We assume that unless weathering has obvious effects on lithophile trace elements (such as U, Sr and Ba), it probably has no major effect on nonchalcophile, highly siderophile elements such as Ni, Ir and Os. Among warm-desert lunar meteorites (Warren et al., 2005) and ureilites (Warren et al., 2006), even in cases where U, Ba and Sr show gross enrichments, Ni, Ir and Os generally appear little-altered.

4. DISCUSSION

4.1. Lithophile-element complexities

A two-component, but otherwise random, model for lithophile-element mixing among HED breccias is in some significant ways oversimplified (Mittlefehldt, 1979). Neither eucrites nor diogenites are compositionally uniform, and their overall compositional range is far from evenly filled by the intermediate-composition polymict breccias (howardites and polymict eucrites). The most pronounced departure from compositional uniformity among the end members involves incompatible elements in eucrites. Including cumulates, the range for Sm extends from 0.067 to 3.7 μg/g (Fig 3b; even excluding cumulates, eucrites range in La over a factor of five). Usui and McSween (2007) improve on the two-component mixing model by setting cumulate eucrite as a 3rd component. However, apart from having consistently near-negligible incompatible element contents in relation to noncumulate eucrites, cumulate eucrites in many ways show greater compositional range intragroup than in comparison with noncumulate eucrites; e.g., for Al_2O_3, MgO and Sc (Fig. 1).

Diogenites show a range for Sc of nearly a factor of five (Fig. 1b), albeit most have 12–16 μg/g. Our six diogenite V determinations (including PCA 02009) appear to represent the first bulk-rock determinations for diogenites, and range from 73 to 320 μg/g. Among these six samples, ALH 77256 (155 μg/g) should be given special weight, because it represents the powder prepared by E. Jarosewich from a large mass (20.6 g) of the meteorite. On Fig. 3a, the howardite mixing trend extrapolated to average diogenite MgO (26 wt%) suggests that the diogenite average V content is roughly 130 μg/g, which agrees as well as could be expected with the direct average (154 μg/g) for the five analyzed diogenites (Table 1). But the scatter among the more MgO-rich howardites also confirms that diogenite V contents must be diverse. Modal and mineral–chemical (SIMS) data for a large suite of diogenites (Bowman et al., 1999; a major repository for V is Cr-spinel, which averages only 0.9 vol% and is heterogeneously distributed even within individual diogenites) likewise imply that bulk-diogenite V contents are probably diverse but average roughly 140 μg/g. Diogenite Cr content is also diverse, ranging from 4.0 (NWA 4272: Barrat et al., 2008b) to 16 mg/g (NWA 4283), and diversity for Cr is commensurately great among MgO-rich howardites, including Melrose (b) with 7.5 mg/g Cr, and Chaves with (despite its high 19.1 wt% MgO) 4.0 mg/g (Fig. EA-1; cf. the different perspective of 8 years ago: Wolf et al., 2001). Among our own six samples, diogenites even show diversity in Al_2O_3 (Fig. 1). Diversity in modal plagioclase, and thus Al_2O_3, is to be expected among small samples from igneous cumulates. Also, Y-75032 and -791200 were selected for study largely because of their unusually high modal plagioclase. As discussed in the Electronic Annex, Y-791200 is a polymict breccia known to contain cumulate eucrite; it is possibly a howardite, and yet (confusingly!) also probably paired with the "monomict" Y-75032.

The great incompatible enrichment diversity among the eucrites manifests only in dampened form among the howardites. The number of well-analyzed howardites is still less than ideal for statistical evaluations, but on Fig. 3b the available data are, with a single exception (LEW 87002), confined to a relatively narrow band within the overall composition-space of eucrites and diogenites. Evidently, either only intermediate-type eucrites (with ~1.1–2.4 μg/g Sm; i.e., excluding cumulates and Sm-rich, Stannern Trend noncumulates) tended to mix with diogenites to form the howardites, or the eucrite component that mixed into the howardites tended to undergo a process of homogenization before the final mixing episode.

A significant cumulate eucrite component is suggested by the slope of the mixing trend on Fig. 1a (a plot of CaO vs. MgO appears very similar). The tightly correlated howardite trend extrapolates to intersect the near-constant MgO (6.8 ± 0.5 wt%) of the noncumulate, non-polymict eucrites (open symbols) at 13.2 wt% Al_2O_3, which is close to, but suggestively greater than, the noncumulate, non-polymict eucrite mean Al_2O_3 of 12.5 wt%. Put another way, of the 49 noncumulate eucrites (including 21 polymict eucrites) with lower MgO than the most MgO-poor howardite (9.2 wt%), only eight fall on the high-Al_2O_3 side of the extrapolated howardite mixing trend. Similarly, on the plot of CaO vs. Sc (Fig. 4), noncumulate CaO-rich eucrites are mostly on the high-Sc side of the extrapolated howardite trend. These trends suggest that the howardites include at least a minor component that is Al_2O_3 and Sc rich, but has far higher MgO/Al_2O_3 and slightly lower Sc/CaO than the average noncumulate eucrite. The cumulate eucrites feature great Al_2O_3 and Sc diversity, but on average (Table 4), they match the requirements of the third component.

However, the overall magnitude of the cumulate eucrite component within the howardites is evidently far subordinate to the noncumulate eucrite component. The howardite Al_2O_3–Sc mixing trend (Fig. 1b) is even tighter than might be expected just from the diversity among noncumulate eucrites. In Fig. 3b, the space between typical diogenite (~26 wt% MgO, extremely low Sm) and the main cluster of cumulate eucrites (7–14 wt% MgO, 0.1–0.5 μg/g Sm) is devoid of howardites.

Table 4
Averaged bulk-rock compositional results for various subcategories of HED meteorite.

Subcategory of HED meteorite	Na_2O (wt%)	MgO (wt%)	Al_2O_3 (wt%)	SiO_2 (wt%)	CaO (wt%)	MnO (wt%)	FeO (wt%)	*mg* (molar)	Sc (μg/g)	Ti (mg/g)	V (μg/g)	Cr (mg/g)	Co (μg/g)	Ni (μg/g)	Ga (μg/g)	Sr (μg/g)	La (μg/g)	Sm (μg/g)	Eu (μg/g)	Lu (μg/g)	Hf (μg/g)	Ir (ng/g)	Au (ng/g)	Th (μg/g)
Pristine-igneous diogenites (29[a])	0.03	26.5	1.13	52.8	1.38	0.49	16.5	74	14.8	0.6	131	6.5	20.6	37	0.20	1.8	0.09	0.07	0.020	0.027	0.07	0.14[b]	0.16[b]	0.014
±	0.03	2.3	0.69	1.7	0.66	0.11	2.2		5.6	0.3	61	3.0	7.4	36	0.10	2.4	0.12	0.08	0.034	0.023	0.07	0.15[b]	0.15[b]	0.017
All pristine-igneous eucrites (35)	0.39	7.8	12.5	49.6	9.9	0.54	18.0	44	28.5	3.4	74	2.7	6.9	2.6	1.3	74	2.5	1.50	0.60	0.23	1.12	0.020	1.7	0.31
±	0.11	2.0	1.6	0.8	0.8	0.06	2.0		3.7	1.6	16	1.2	2.8	2.9	0.4	16	1.6	0.87	0.17	0.10	0.62	0.034	4.0	0.18
Pristine noncumulate eucrites (26)	0.44	6.8	12.6	49.4	10.1	0.55	18.7	39	29.8	4.0	69	2.3	5.8	2.3	1.4	74	3.0	1.78	0.67	0.28	1.30	0.027	2.2	0.33
±	0.07	0.5	0.9	0.7	0.2	0.04	0.7		2.1	1.2	11	0.3	1.5	2.8	0.4	15	1.3	0.66	0.10	0.06	0.48	0.040	4.6	0.16
Pristine cumulate eucrites (9)	0.27	10.7	12.1	50.0	9.2	0.51	16.0	54	24.8	1.9	89	4.0	10.0	3.5	1.0	72	1.12	0.68	0.42	0.11	0.54	0.008	0.34	0.20
±	0.11	2.1	2.6	0.9	1.2	0.08	3.0		4.7	1.5	17	1.7	3.2	3.0	0.4	18	1.61	0.86	0.18	0.11	0.65	0.011	0.52	0.25
Polymict eucrites (34[a])	0.42	8.7	11.7	49.6	9.3	0.52	18.2	46	28.1	4.0	74	3.0	12.2	77	1.3	64	2.8	1.64	0.59	0.25	1.25	3.9	8.8	0.35
±	0.07	1.9	0.9	0.5	0.7	0.03	0.9		2.6	1.0	17	0.9	16.8	222	0.4	15	1.2	0.65	0.11	0.07	0.43	8.2	27.8	0.19
All howardites (40[a])	0.26	15.5	7.8	50.3	6.4	0.51	17.6	61	22.4	2.4	98	4.9	23.8	277	1.0	44	1.68	1.01	0.36	0.16	0.72	9.4	6.2	0.16
±	0.07	2.9	1.9	1.0	1.4	0.03	1.0		2.8	0.6	15	1.2	14.2	481	0.7	15	0.54	0.30	0.08	0.04	0.18	11.6	8.5	0.06
Regolithic howardites (5[c])	0.32	14.0	8.8	49.5	7.0	0.51	18.2	58	24.7	2.6	93	4.3	35.1	503	1.3	59	1.74	1.04	0.38	0.17	0.78	23.0	7.6	0.22
±	0.04	1.2	0.6	0.6	0.6	0.01	0.9		2.0	0.4	9	0.4	8.1	183	0.2	16	0.27	0.12	0.05	0.01	0.13	7.8	2.7	0.02

Averages are based on the same data sets used in the figures; i.e., mainly from this work, but supplemented, as described in the text, with literature data for 24 diogenites, 10 howardites (see Table EA-5), four pristine-igneous eucrites and one polymict eucrite (the impact-melt breccia NWA 1240). The "Mg-rich" EET 87520 has been averaged as a noncumulate eucrite. The "±" rows list one-sigma standard deviations.

Note: the listing of standard deviations for all elements is meant to convey a sense of the variance (often very large!) for the element-sample-type combination, not to suggest that any element's distribution is gaussian.

[a] Weathered samples were excluded from the averaging for incompatible elements, Sr and CaO.

[b] For Ir and Au in diogenites, only data from this work are included in the averages.

[c] The regolithic howardite category is here defined conservatively as the 4 gas-rich howardites (Bholghati, Bununu, Jodzie, Kapoeta) plus Malvern, which appears to have once been gas-rich (Kirsten and Horn, 1977).

For comparison, a rough estimate for the relative proportions of cumulate to noncumulate eucrite may de derived from simple statistics on the numbers of individual unbrecciated or monomict-brecciated eucrites that have been characterized sufficiently well to draw this distinction. This ratio currently stands at roughly 15:60, or 0.25, for cumulate:noncumulate eucrites. Caveat: there may be a slight observational bias; petrologists and geochemists may have over time put greater efforts into characterizing the rarer and more diverse type, i.e., cumulates.

Another approach to estimating the relative proportions of cumulate to noncumulate eucrite stems from evidence that most of the noncumulate eucrites originated as part of the Nuevo Laredo trend (e.g., Fig. EA-3, which is our version of a similar plot by Gardner and Mittlefehldt, 2004). In the Nuevo Laredo trend, only moderate incompatible-trace-element variation is seen in conjunction with variations in other differentiation markers such as the *mg* ratio (Warren and Jerde, 1987) and Sc (Gardner and Mittlefehldt, 2004). As discussed by Warren and Jerde (1987) and Gardner and Mittlefehldt (2004), this type of fractionation pattern suggests a fractional crystallization process in which cumulate eucrite crystallizing and segregating from the melt drove the fractionation. However, only a moderate degree of fractionation is recorded. Based on La (an almost ideally incompatible element), an average Nuevo Laredo trend sample (2.83 μg/g) is only enriched by a factor of roughly 1.2–1.4 over the low-La end of the trend. (Caveat: The low end of the N.L. trend is uncertain. Even the membership of the N.L. trend is uncertain. For the trend's central, "Main Group" members, it is hard to rule out overlap with the other noncumulate eucrite trend, the Stannern trend, which shows the strong incompatible element variation expected in a partial melting sequence.) The proportion of cumulate that would engender an average La enrichment factor of 1.2–1.4 is 20–40%. After correcting for the additional component of Stannern trend eucrites (roughly 20% of all noncumulates), this model leads to an estimate for the overall cumulate:noncumulate eucrite ratio of roughly 0.2–0.3. The result by this approach is thus similar to that from simply tallying up the well-characterized eucrites. The howardite and polymict eucrite evidence (Figs. 1–4) is broadly consistent with both of these estimates derived from the unbrecciated and monomict-brecciated eucrites.

4.2. Siderophile and siderophile-related constraints on the mixing process

Not surprisingly, polymict-HED breccias show a strong correlation between Ni and the arch-siderophile Ir (Fig. 6a). The predominant type of chondritic matter found as clasts in HED meteorites is CM (Zolensky et al., 1996), and the Ni/Ir trend almost precisely matches the ratio (20,000) of average CM chondrite (Wasson and Kallemeyn, 1988; chondritic Ni/Ir ranges from 16,600 in CK to 31,000 in EH).

In the pristine-igneous HED samples, Ni/Ir is almost uniformly superchondritic, averaging ~52,000; and by siderophile standards the ratio seems fairly consistent, from the extreme low-Ir end of the trend (eucrites such as EET 87542 and LEW 87010) to the high end (diogenite NWA 1461). This enrichment in Ni/Ir by a factor of ~2.5 in the mantle + crust component of the HED-parent asteroid is mild compared to the enrichment factors inferred for larger bodies, such as ~7 for Mars, 30 for the Moon, and 37 for Earth (Warren et al., 1999). This suggests near-complete partitioning of both Ni and Ir into the nascent core of the parent asteroid, an outcome that may require that the asteroid's deep interior was at one time mostly molten (cf. Righter and Drake, 1997).

The correlation between Ni and Co (Fig. 6b) is not so linear, because pristine-igneous HED materials contribute enough Co to significantly affect Ni/Co in all but the most siderophile-rich of the polymict compositions. The polymict eucrite QUE 97004 is mysteriously Co-rich. The pristine-igneous eucrite Nuevo Laredo (Warren and Jerde, 1987; cf. BVSP, 1981; Barrat et al., 2007) and the Lohawat howardite (Sisodia et al., 2001) are strangely Co-poor.

More often than not, when howardites are defined they are said to be (as a class) regolith breccias (e.g., Fuhrman and Papike, 1981; Warren, 1985; Gounelle et al., 2003; Wiechert et al., 2004; Mittlefehldt, 2005; Lorenz et al., 2007). Sometimes the description of the howardite group is more nuanced. For example, Bischoff et al. (2006) considered 8/21 howardites to be "gas-rich" and thus, by their definition, regolith breccias. However, their definition for "gas-rich" was not specified (it also is unclear how pairing, such as among the many and widely analyzed Yamato howardites, was addressed). Hewins (1982), in full cognizance of basically the same noble gas database, argued that howardites, as a class, are "ejecta deposits, not soils." In part, this range in opinion arises because definitions used for regolith breccia are inconsistent and context-dependent. Regolith is often defined broadly as, e.g., "a (surface) layer or mantle of loose, rocky material of whatever origin" (Housen and Wilkening, 1982). Lucey et al. (2006, p. 84) give a similar definition, and note that every lunar rock ever acquired (at least, every non-meteoritic lunar rock) is "from the regolith"; and thus, one might assume, any lunar breccia sample should be a regolith breccia. Instead, at least in the lunar context, regolith is in practice taken to mean the soil-like material that has been efficiently impact-gardened down to *the scale of individual mineral grains* – which, in lunar rocks, are seldom much more than 1 mm across. The Moon's "true regolith" (McKay et al., 1991, p. 286) is thus only about 5–15 m thick, even though the body's outer few kilometers are believed to be a loose pile of impact ejecta-rubble (megaregolith). Of course, another complication is that even the "true" regolith is rich in (in a sense, broken up by) surviving lithic fragments, sometimes of great size. In lunar petrology, rocks are only termed "regolith breccia" if they appear to have formed, at least for the most part, as a parcel of the "true," soil-like regolith.

Only a minor subset of howardites have noble gas enrichments or petrographic indications (i.e., abundant glasses, especially spheroidal or "turbid" brown (agglutinitic?) glasses: Olsen et al., 1990) suggestive of "true" regolith derivation. Glass/spheroid abundance data are seldom reported in quantitative form. Also, a few spheroids occur even in polymict eucrites such as FRO 97045 (Grossman,

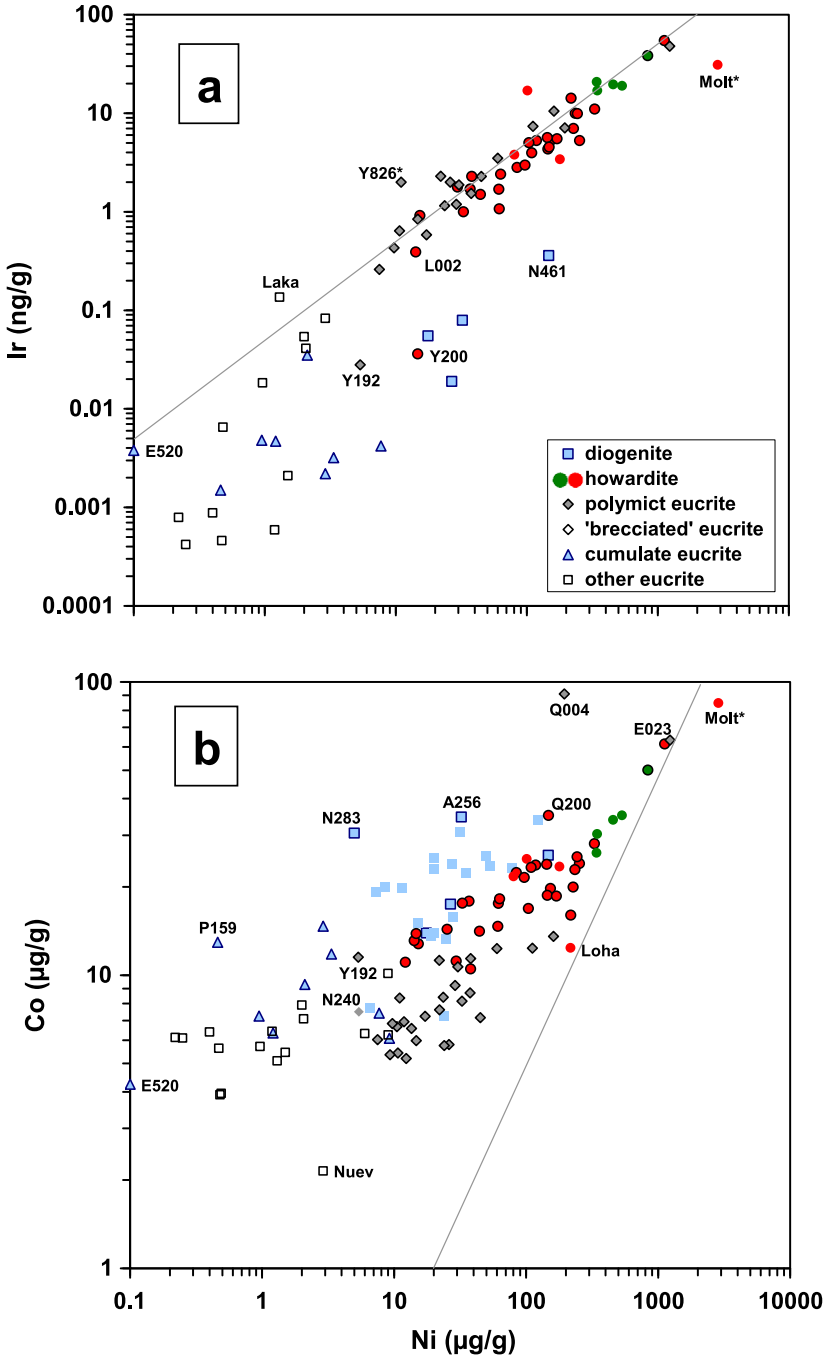

Fig. 6. Siderophile element variations among HED meteorites: bulk-rock Ni vs. (a) the arch-siderophile Ir, and (b) the mildly siderophile Co. The dataset for Ir in diogenites is restricted to results from this lab. The abbreviations for Molteno and Y-791826 include asterisks because the plotted compositions are problematical. Y-791826 is a case where our data for both Ni and Ir (Table 2) are extraordinarily uncertain. In the case of Molteno, the literature data represent analyses for Co, Ni and Ir using separate chips (Frost, 1971; Laul et al., 1972; Palme et al., 1983). Molteno's true composition is probably close to that shown but nearer to the diagonal lines, which indicate the Ni/Ir and Ni/Co ratios of CM chondrites (Wasson and Kallemeyn, 1988). Regarding symbols and data sources cf. Fig. 1.

2000); and in some lunar breccias that are generally classified as fragmental, not regolithic, breccias (e.g., Y-82192/86032: Bischoff et al. 1987; Takeda et al. 1990). Incidentally, Olsen et al. (1990) argued that HED meteorites rich in spheroidal glasses could only form on an asteroid with diameter at least 800 km, i.e., distinctly larger than Vesta's d of ~540 km (Thomas et al., 1997). Only on such a large asteroid could an appreciable fraction of impact ejecta, including spheroids, be expected to fall back onto the asteroid surface, Olsen et al. (1990) assumed. However, the premise for this assumption is traceable to a model of collisional effects on asteroids (Davis et al., 1979; Kluger et al., 1983)

that unrealistically assumed solid-rock-like target properties for the asteroid's shallow interior. More realistically (Housen and Wilkening, 1982), collisional evolution creates a brecciated interior that responds to impacts in a more subtle way than assumed by Davis et al. (1979). Recent spacecraft observations have left no doubt that asteroids much smaller than Vesta develop substantial regoliths (Richardson et al., 2005).

For interpretation of the noble gas data, one complication is that the solar wind flux in the asteroid belt is, by the inverse-square law (e.g., Housen and Wilkening, 1982), about 0.1–0.2 times the flux at 1 AU. For Vesta, at 2.36 AU, the inverse-square factor is 0.18. If, as Zahnle (2006) inferred, the early solar-wind flux underwent an exponential decline with half-life of 320 Ma, even the timing of the regolith gardening might be significant. Most of the Apollo regolith samples developed by impact-gardening only in the last 3.9 Ga (upon terrains that were resurfaced by fresh mega-impact ejecta, if not mare-basaltic lava, at least as recently as the age of Imbrium). The impact-gardening that engendered the howardites probably occurred largely (mostly?) before 3.9 Ga (Bogard, 1995).

As reviewed by Shukolyukov et al. (2001) and Lorenzetti et al. (2005), mature lunar regolith samples, such as the meteorites ALH 81005, DaG 262, QUE 93069, QUE 94281, Y-791197 and Y-793274, contain 100–1000 nl/g of ^{20}Ne (nl stands for nanoliters; meteorite noble gas concentrations are traditionally reported in units of vol/g at STP, standard temperature and pressure). Very low-maturity samples that are nonetheless unambiguously regolith breccias, such as MAC 88104 and Dhofar 025, contain typically ~1 nl/g. However, some fragmental, non-regolith lunar breccias contain well over 1 nl/g. For example, the polymict breccia lunaite Dhofar 081 contains 1–4 nl/g of ^{20}Ne (Greshake et al., 2001; Shukolyukov et al., 2001). Yet Dhofar 081 is usually classified as a fragmental breccia (see Warren et al., 2005, who, however, argued that Dhofar 081 evidently has a significant regolith component and might be better classified as an immature regolith breccia). The EET 96008 breccia, which is clearly fragmental, not regolithic (Warren and Kallemeyn, 1989; Anand et al., 2003), contains ~4 nl/g (average including data from Vogt et al., 1993).

For comparison, based on literature-averaged data (Fig. 7), only four howardites are known to contain more than 0.2 nl/g of ^{20}Ne – the Vesta-to-Moon equivalent of 1 nl/g. Another three howardites are marginally "enriched" by ~0.1 nl/g (lunar equivalent: 0.5 nl/g), but most howardites contain no more ^{20}Ne than a typical diogenite. The four clearly gas-rich howardites (Kapoeta, Jodzie, Bununu and Bholghati) also feature relatively high siderophile contents, e.g., higher in Ir than all but one of the gas-poor howardites (and none of the known gas-poor polymict eucrites). However, the most Ni-rich howardite, Molteno, is not (based on a single noble gas study) gas-rich.

Allowing for the inverse-square decline of solar-wind flux (assuming Vesta as the source body), the most gas-rich howardite is still a factor five less rich in noble gases than a

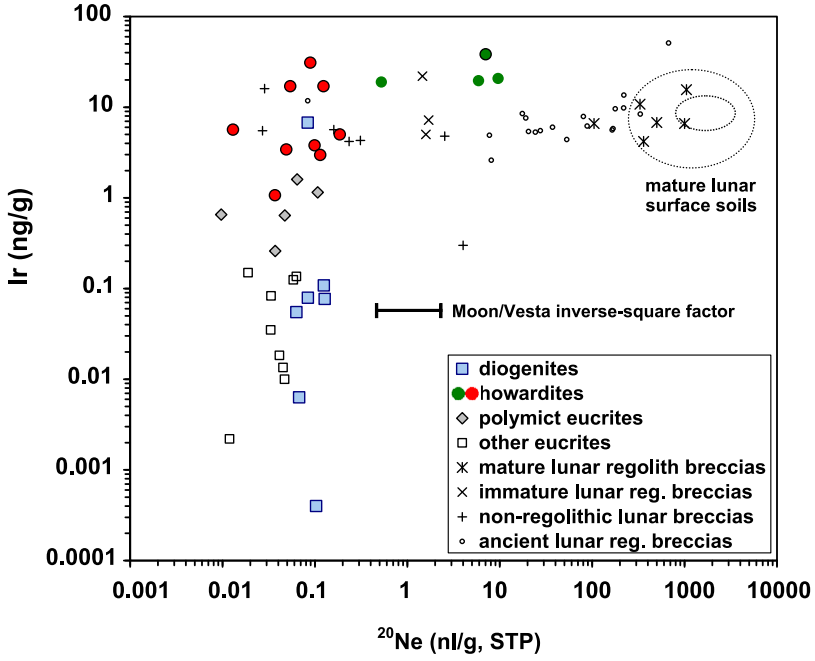

Fig. 7. Noble gas vs. siderophile contents of HED meteorites. The HED ^{20}Ne data are mainly from the compilation of L. Schultz (e.g., Patzer et al., 2003). ^{20}Ne is representative of a large variety of noble gas isotopes that are enriched in the solar wind and strongly correlated with one another among gas-rich meteorites. Lunar breccia ^{20}Ne data are from lunar meteorite reviews by Shukolyukov et al. (2001) and Lorenzetti et al. (2005), and from McKay et al. (1986) for the ancient Apollo 16 regolith breccias. The field for mature lunar surface soils is based on the compilation of Walton et al. (1973; the inner field delineates the range among pre-averaged data for 7 landing sites; the outer field includes a few samples that McKay et al. (1991) would term "submature"). The database used for Ir in lunar samples is essentially that of Warren (2004).

typical lunar mature regolith. As noted by Housen and Wilkening (1982), the higher cratering rate in the asteroid belt (ignoring potential temporal variation) inevitably causes more rapid turnover of surface layers, so the maximum gas level observed (Fig. 7) may be virtually as high as ever developed on Vesta.

Howardites also show a correlation between siderophile abundance and major-element composition (Fig. 2). Although loose, this correlation is clearly significant. For the 19 howardites (including well-determined literature compositions) with Al_2O_3 lower than the howardite mean (7.8 wt%: Table 4), average Ni content is 91 μg/g. For the 21 with >7.8 wt% Al_2O_3, average Ni content is 450 μg/g. Conceivably the true average Ni for the higher-Al_2O_3 group is even higher; the four outstandingly low-Ni samples include Hughes 004 and Melrose (b), in which the low Ni is conceivably a result of warm-desert weathering; and EET 96003 and EET 99408, which are quite possibly, in view of this shared unusual trait, paired. Also, although the eucritic component contributes very little Ni, the lower-Al_2O_3 half of the howardite trend includes significant Ni (~27 μg/g) from its large (average ~55%) diogenitic component; i.e., only about 2/3 of the 91 μg/g stems from impactor contamination.

Of the nine howardites with >300 μg/g Ni, seven have Al_2O_3 confined to 8–9 wt% (and the outliers, Malvern with 9.9 wt% and MAC 02666, with 11.5 wt% Al_2O_3, barely qualify as Ni-rich). Conceivably, this clustering near 8–9 wt% Al_2O_3 is merely an artifact of the limited number of analyzed samples. However, the set of 9 high-Ni howardites includes all four of the unambiguously gas-rich howardites (Fig. 7). For the other five Ni-rich howardites, in three (Muckera 001, LEW 85313 and MAC 02666) the gas content is unknown. Although Malvern is gas-poor, it is exceptionally rich in "turbid" (regolithic?) brown glass (Olsen et al., 1990). In fact, Malvern has heavily annealed solar flare tracks (of presumed regolithic origin), and details of its noble gas isotopic pattern suggest it was originally rich in gases but lost them through annealing (Kirsten and Horn, 1977). If so, of the six Ni-rich and gas-analyzed howardites, only Molteno, which is in a sense overly siderophile-rich (far more siderophile-rich than any lunar regolith breccia: Haskin and Warren, 1991), is known to never to have held enrichments in solar noble gases. The compositional clustering of the regolithic howardites is particularly impressive in view of their comparative immaturity, by lunar standards (Fig. 7). In terms of maturity, they seem more closely analogous to typical lunar regolith breccias (McKay et al., 1986) than to lunar soils, per se.

Besides solar gases, glasses and Ni, the gas-rich howardites are also distinctively rich in carbonaceous chondrite clasts. A search for such clasts in "all available sections of howardites and eucrites" at five of the world's top repositories of meteorites led Zolensky et al. (1996) to note (with slight hyperbole) that, compared to Kapoeta and Jodzie, other HED breccias are "totally devoid" of recognizable carbonaceous chondrite clasts. Buchanan et al. (1993) also described 18 carbonaceous chondrite clasts from Bholghati.

The relationship between Ni content and gas enrichments was noticed long ago by Hewins (1982). However, Hewins was not aware of the tendency for these Ni- and gas-rich howardites to cluster in major-element composition near 8–9 wt% Al_2O_3 – a remarkably tight cluster, when viewed in comparison to the overall distribution of howardite compositions, evenly spread across the range 4.6–11.5 wt% (Fig. 2). Of the nine howardites with >300 μg/g Ni, the two least likely to be regolithic are the extremely Ni-rich Molteno (known to be gas-poor) and MAC 02666, about which little is known, but it has the lowest Ni of the group (330 μg/g), by far the lowest Ir (11 ng/g) and also the most outlying lithophile composition: high in Al_2O_3 (11.5 wt%) and Sm (1.5 μg/g), low in MgO (9.3 wt%) and Cr (2.9 mg/g).

The Ni and Ir contents of howardites and polymict eucrites, as populations, are compared with those of lunar regolith breccias and lunar non-regolithic impactites in Fig. 8, where the database used for lunar samples is essentially that of Haskin and Warren (1991). In this figure, the *x*-axis is shown as a probability scale (i.e., probability corresponding to the normal distribution; such that ideally log-normal distributions would plot as straight lines). Again, we will concentrate our discussion on Ni, because the present database for Ir in polymict eucrites is inadequate (too many upper limits) to constrain the trend beyond the most Ir-rich 15% of the population. The population of howardite Ni contents is not a close match to the population of lunar regolith breccias. The median Ni contents are roughly similar (248 and 118 μg/g, for lunar regolith samples and howardites, respectively). But howardite Ni contents are far more diverse: 37% are lower in Ni than the most Ni-poor lunar regolith sample. The howardite pattern shows a fair resemblance to the pattern for lunar non-regolithic polymict impactites (i.e., mostly polymict breccias but including a few impact-melt rocks that appear unbrecciated), except over most of its breadth the howardite pattern is displaced to lower Ni by a factor of ~2. Still, if the subset of five howardites with gas enrichments (or, in the case of Malvern, evidence of former gas enrichments) is regarded as a separate but woefully undersampled (caveat!) population, these HED regolith breccias feature higher median Ni and Ir contents, in comparison to lunar regolith samples, by a factor of roughly two.

The polymict eucrites are remarkably Ni-poor, as a population, compared to lunar non-regolithic impactites. Over most of its breadth the polymict eucrite pattern is displaced to lower Ni by a factor of ~10. Conceivably, to a slight extent, this may reflect higher Ni in the pristine-igneous lunar crust compared to pristine eucrites. However, the polymict eucrite pattern remains lower in Ni by a similar factor (about 8–10) even for the portion of the Ni-concentration spectrum where the lunar samples contain 200–1000 μg/g Ni, which is presumably not to any significant extent of pristine-igneous derivation (cf. Warren et al., 1999, and discussion of Fig. 6a, above). The low-Al_2O_3 howardites are similarly siderophile-poor (Fig. 2; bearing in mind that at the low-Al_2O_3 end of the howardite trend the mixtures probably obtain several tens of μg/g Ni from their pristine-igneous diogenite components).

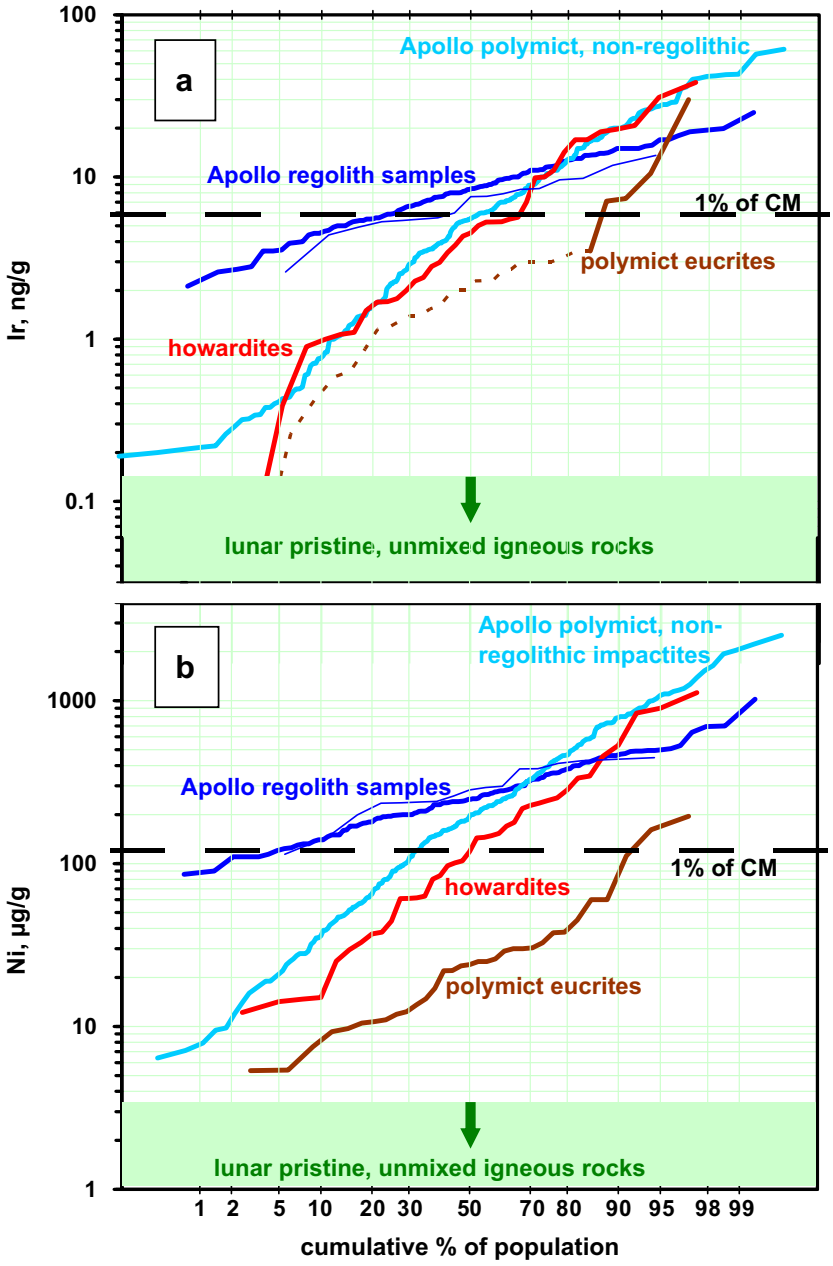

Fig. 8. The (a) Ir and (b) Ni contents of howardites and polymict eucrites, as populations, compared with those of regolith breccias and non-regolithic impactites from the Moon. For Ir (a), most of the polymict eucrite population is represented only by series of upper limits, shown as the dotted curve, because in most cases only upper limits are available for the individual meteorites. On both diagrams, the thin but continuous dark blue curve represents the subpopulation of ancient regolith breccias identified by McKay et al. (1986); its pattern of Ni and Ir enrichment is similar to that of lunar regolith samples in general. (For interpretation of color mentioned in this figure, the reader is referred to the web version of this article.)

The patterns in the case of Ir (Fig. 8a) are similar. The howardite Ir spectrum displays great diversity compared to that of lunar regolith breccias, and more closely matches the pattern of the lunar non-regolithic polymict impactites. The polymict eucrite Ir spectrum is poorly constrained, but the data again suggest systematically much lower siderophile enrichments than are prevalent among lunar polymict impactites. Note that the subset of 18 "ancient" (and mostly immature) Apollo 16 regolith breccias identified by McKay et al. (1986) are little different, in terms of Ni and Ir, from the general population of mostly recent lunar regoliths. If anything, the ancient regoliths appear to feature higher Ni/Ir, averaging ~2.1× (CM) chondritic. However, this probably has more to do with location than timing or regolith maturation. Modern, mature Apollo 16 soils also average ~1.7× chondritic Ni/Ir (database of Haskin and Warren, 1991; cf. Korotev, 1987).

Unfortunately, the database for siderophile elements in polymict diogenites seems to be limited to two meteorites. Mittlefehldt's (1994) analysis of a 42 mg piece of the notoriously heterogeneous Aioun el Atrouss shows 2 ng/g Ir but only 40 μg/g Ni (i.e., less than an average pristine-igneous diogenite: Table 4). In Garland, Mittlefehldt (1994) did not detect Ni, but Wolf et al. (1983) found 26–29 μg/g, and Ir so low (0.07–0.08 ng/g) that, in the lunar context, the rock might be interpreted as compositionally pristine. These scant available data suggest that like polymict eucrites, polymict diogenites tend to be siderophile-poor compared to lunar polymict impactites.

Summing up the siderophile and siderophile-related constraints, only a few howardites, and none of the polymict eucrites, appear to be regolith breccias in the sense that this term is commonly applied in lunar petrology. To distinguish this important subset of gas-, glass- and Ni-rich howardites that appear to be regolith breccias, we propose that they be termed *regolithic howardites*. The regolithic howardites appear to have Al_2O_3 contents strongly clustered toward 8–9 wt%. Among polymict eucrites (and probably also polymict diogenites), siderophile enrichment levels tend to be vastly lower than in lunar polymict impactites.

4.3. Brecciation-mixing on the HED asteroid

If our sampling is reasonably representative, we have three intriguing clues to the history of impact brecciation-mixing on the HED-parent asteroid.

1. The clustering of the regolithic (gas-, glass- and Ni-rich) howardites near 8–9 wt% Al_2O_3 implies that some aspect of the geology of the parent asteroid's crust caused "true" regolith to only develop by mixing of ~2:1 (eucrite:diogenite) proportions of the two petrologically opposite rock types. Neither mostly diogenitic, nor near-pure eucritic, regolith breccias are common.
2. Another peculiar aspect of the HED mixing trends concerns the frequency for breccias to be polymict as opposed to monomict. Based on the on-line Meteoritical Bulletin database maintained by J.N. Grossman, only eight of the 182 named diogenites are polymict breccias, even though virtually all the rest are monomict breccias (and foreign matter should be especially easy to spot in this near-monomineralic rock type). In contrast, of 234 named, brecciated eucrites that have been classified as either monomict or polymict, 140 (60%) are polymict.
3. Finally, the mixing that engendered the polymict eucrites and the low-Al_2O_3 howardites imparted, in most cases, remarkably mild siderophile enrichments.

Constructing a model to account for all these peculiarities is a challenge. Cogent dynamical evidence suggests that Vesta, through its family of dynamically linked and basalt-surfaced vestoids, is the ultimate source of the HEDs (Binzel and Xu, 1993). Only one other basalt-surfaced belt asteroid has been observed (Hardersen et al., 2004), and the Vesta-HED hypothesis has won general acceptance (e.g., Righter and Drake, 1997; Gaffey, 1997; Keil, 2002; Usui and McSween, 2007). Wasson et al. (1996) argued that the Vesta-HED link is not definite. The known, surviving vestoids include one for which estimates of d range up to ~14 km (Kelley et al., 2003) and ~12 others with d of 5–10 km (Binzel and Xu, 1993; Burbine et al., 2001). Ejection of such large masses off Vesta requires an extraordinarily large impact. The minimal space weathering of Vesta's surface (Binzel et al., 1997) strongly suggests that the resurfacing associated with this great impact happened at an uncommonly late date. Modeling by Asphaug (1997), a supporter of the Vesta-HED link, indicates that an impact large enough to make the largest known vestan crater ($d \sim 460$ km: Thomas et al., 1997) can be expected to launch a single fragment 15 km in d but no other with $d > 2.6$ km and only a total of three with $d > 1.6$ km.

Wasson et al. (1996) proposed that the surfaces of the vestoids may appear basaltic only because a recent large and oblique impact on Vesta caused all asteroids in its dynamical vicinity to become coated with a misleading veneer of Vesta-dust. Another cause for mild concern regarding the Vesta-HED hypothesis is that according to Gaffey's (1997) modeling of Vesta spectral data, the average regolithic pyroxene composition is $\sim En_{46}Fs_{46}Wo_8$; the uncertainty in the En proportion is estimated to be "of order" 10 mol%. The only samples that plausibly represent the surface regolith of Vesta are the howardites, and especially the regolithic (gas-, glass- and Ni-rich) howardites that, as discussed above, consist of about 1/3 diogenitic and 2/3 eucritic debris. (We argue below that the great, late impact that launched the vestoids probably altered the global surface of Vesta. The most likely effect of such a great impact, in terms of the surface diogenite:eucrite ratio, was to enhance the global surface proportion of excavated deep origin material, i.e., diogenite.) In a 1/3 diogenitic, 2/3 eucritic howardite, the pyroxene is almost as much diogenite-derived as eucrite-derived (diogenites are nearly 100% pyroxene; eucrites only about 60%: BVSP, 1981). Diogenitic pyroxene is generally close to $En_{74}Fs_{24}Wo_2$ (Fowler et al., 1994). Eucrite pyroxene is diverse but probably (including cumulates) averages at least as magnesian as $En_{41}Fs_{49}Wo_{10}$ (an average pristine-igneous eucrite, despite contributions from high-Fe/Mg minor phases such as ilmenite, spinel and FeS, has bulk $mg \sim 44$ mol%: Table 4). The samples thus suggest that the surface regolith's average pyroxene should be about $En_{55}Fs_{38}Wo_7$, for which Gaffey's (1997) Vesta estimate gives only a marginally acceptable match. A slightly more magnesian, but also more Ca-rich, pyroxene composition ($En_{51}Wo_{12}$) has been inferred by Kelley et al. (2003) for the large vestoid Kollaa. But a better match is provided by the estimate of $En_{56}Fs_{36}Wo_8$ for the surface pyroxene of the Vesta-unrelated, ~30-km diameter basaltic asteroid Magnya (Hardersen et al., 2004). However, the preponderance of evidence still appears to favor Vesta as the ultimate source of HED meteorites.

Hubble Space telescope studies of Vesta indicate that its surface is far from uniform, with a large orthopyroxene + olivine region dominating one hemisphere, and basalt dominating the other (Gaffey, 1997; Binzel et al., 1997); implying that the regolith of modern Vesta is highly diverse in Al_2O_3. This raises a paradox, because the regolithic

howardites have Al_2O_3 strongly clustered about 8–9 wt%. Possibly the paradox merely reflects poor sampling of Vesta by the meteorites (or even fallacy of the Vesta-HED hypothesis). But another explanation is that the ancient regolith that spawned the regolithic howardites was much more thoroughly blended than the modern regolith. The general effect of impact-gardening is to increasingly homogenize planetary surfaces. But conceivably an extraordinarily large and late impact on Vesta caused most of the ancient regolith to be either spalled off the asteroid or buried under (and dispersed within) a thick layer of fresh ejecta; and the modern regolith that developed since the impact is far less homogeneous than its ancient predecessor.

For Vesta, an extraordinarily large and late impact is not speculation. Dynamical evidence indicates that the Vesta-family asteroids formed when a large impact (or impacts) spalled them off Vesta probably within the last 1 Ga (Marzari et al., 1996). The largest known crater on Vesta is ~460 km in d (Thomas et al., 1997), and as mentioned above, even this is only dubiously large enough (Asphaug, 1997) to account for launch of ~13 vestoids >5 km in d. Thomas et al. (1997) estimate that the volume of ejecta from the $d \sim 460$ km crater was $\sim 1.2 \times 10^6$ km^3. Assuming Vesta's $d = 540$ km, and that roughly 20% of the ejecta escaped from Vesta (Thomas, 1999), the impact covered Vesta with a layer of freshly excavated rock debris ~1 km thick (on average, ignoring additional volume generated by churning associated with distal secondary impacts). By sheer burial as well as churning, this ejecta-deposition event probably efficiently removed from the surface whatever ancient (regolithic howardite-like) regolith was not directly spalled off by the primary impact. Such a model may also explain the curious observation that vestoid surfaces consistently appear more "red" (i.e., more space-weathered, more "mature") than the surface of the vastly larger and older Vesta (Burbine et al., 2001).

The late impact that spalled off the vestoids (probably our only source for HED meteorites) undoubtedly yielded new brecciation-mixing on Vesta, but the generation of mixed breccias from that event are probably extremely rare among the available (vestoid-derived) samples. The martian meteorites are in some ways analogs of the vestoids. Each martian meteorite underwent a recent launch impact, analogous to the comparatively recent (Marzari et al., 1996) vestoid-forming impact. Even though these late-launch impacts induced maskelynitization (Mars' v_{escape} is extremely high, by asteroid standards), they did not launch newly produced polymict breccias, or reset conventional age-dating systems. Apart from cosmic-ray exposure ages, it would be impossible to use isotope geochronology to constrain when the martian-launch impacts happened (Nyquist et al., 2001).

Even assuming the regolithic howardites represent a distinct earlier phase of vestan regolith development, their clustering near 8–9 wt% Al_2O_3 is enigmatic. Both HED sample-petrologic (e.g., Fowler et al., 1994; Mittlefehldt, 1994; Keil, 2002; Zema et al., 1997) and Vesta remote-sensing (Gaffey, 1997) observations indicate that pyroxenitic (diogenitic) material generally formed deeper than basaltic (eucritic) matter. Various lines of evidence, including the remote observations, and the simple assumption that a chondritic, ~10%, complement of feldspar managed, along with a similar, eutectic proportion of pyroxene, to efficiently differentiate into its gravitationally favored position as the uppermost layer of the interior, suggest that the eucritic crustal layer is several tens of km thick (Ruzicka et al., 1997; Warren, 1997). But if so, and if the correlation between depth and diogenite/eucrite ratio was originally strong, then only a small minority of craters should be large enough to excavate into the deeper pyroxenite, and regolith diogenite/eucrite ratio (i.e., Al_2O_3) might vary widely depending upon location in relation to those few large craters. To some extent that diogenite/eucrite ratio diversity may be underrepresented among vestoid-derived HEDs. The giant basin that putatively launched the vestoids has a d 0.27 times the circumference of Vesta (Thomas et al., 1997), but the source region for ejecta launched fast enough to become vestoids (Asphaug, 1997) was presumably much smaller than that. Still, the howardite evidence may be an indication that the real structure of the vestan interior was never so simply and neatly layered, so that the correlation between depth and diogenite/eucrite ratio is weak.

However, an alternative scenario is to recognize that the largest 1–2 impacts experienced by any given planet can be vastly larger than all others (i.e., the premise for the giant impact model of lunar origin). The diogenitic material added to the ancient (pre-vestoids) surface may have been entirely excavated by just one exceptionally large and early crater. If subsequent cratering involved no impacts (apart from the ~1 Ga vestoid-forming, surface-resetting impact) large enough to excavate additional diogenite, and yet the impacts were numerous and large enough to achieve efficient lateral mixing (possibly advantaged by Vesta's low gravity and high surface curvature), then the clustered Al_2O_3 of the regolithic howardites could be consistent with the petrologically well-layered interior model. Even with efficient lateral mixing, the precise final Al_2O_3 of any given parcel of the ancient regolith would likely anticorrelate with proximity to the diogenite-excavation crater; i.e., the thickness and diogenite/eucrite ratio of the ejecta layer. (But probably not to nearly the same the degree that the Al_2O_3 of the modern regolith, developed only over the last <1 Ga, is governed by proximity to the great vestoid-forming impact.)

The very low proportion of polymict diogenites, in contrast to the abundance of polymict eucrites, is also difficult to explain unless most of the diogenite input to the near-surface (i.e., potentially meteorite-productive) region was accomplished by a very small number of impacts. If the diogenite component was originally not much deeper than the eucrites, and was brecciated in a piecemeal way by numerous different impacts, the outcome would probably be a polymict/monomict breccia ratio similar to that observed among the eucrites. Instead, considering that the diogenites may have originated in a distinct layer beneath the crust (whereas most eucrites, on textural grounds, originated as components of wide but vertically very localized near-surface flows or shallow intrusions), the brecciation of the sampled diogenites may have occurred mainly at depth, where admixture was limited to similarly deep materials (i.e., yielded monomict-diogenite breccias) during a

few unusually large early impacts. Some polymict diogenites would still have formed in the extraordinary event (one, or perhaps two, exceptionally large impacts, as suggested to account for the Al_2O_3 clustering of the regolithic howardites) that excavated the diogenites and dispersed them over the surface of the parent asteroid; and a few diogenites would be brecciated in subsequent small-scale impacts, or even in the vestoid-forming impact. But the ultimate proportion of polymict diogenites would not be as large as implied by piecemeal small-crater excavation from shallow original locations. In this sense, the scarcity of polymict diogenites may be a confirmation of the common assumption (e.g., Takeda, 1979; Warren, 1985, 1997; Righter and Drake, 1997; Ruzicka et al., 1997) that the diogenites originated as a deep global layer of pyroxenite, as opposed to a dispersed mélange of scattered crustal pyroxenitic intrusions (Shearer et al., 1997).

The modest siderophile enrichment levels that characterize most polymict eucrites and low-Al_2O_3 howardites (Fig. 2; and probably also the polymict diogenites) are highly enigmatic. As one possible explanation, we suggest that the polymict eucrites and low-Al_2O_3 howardites may be mostly first-generation impact breccias; and first-generation polymict impact breccias, especially on a small body such as Vesta, may feature only spotty siderophile enrichments. Planetary-dynamical theory (e.g., Farinella and Davis, 1992) implies that impact velocities tend to be much slower, and impacts much gentler, on the HED asteroid than on the Moon. This disparity is confirmed by shock-level statistics (Bischoff et al., 2006) and by the survival of hundreds of known carbonaceous chondrite impactor clasts (mostly CM; e.g., Buchanan et al., 1993; Zolensky et al., 1996; Gounelle et al., 2003) within HED polymict breccias. Within the large and well-studied collection of lunar polymict materials only two chondritic clasts have been found (Zolensky et al., 1996; Rubin, 1997). Another effect of the comparative gentleness of HED collisions may be a tendency for siderophile-rich impactor debris to be less thoroughly disseminated during individual HED impacts. Over time, through repeated impacts, the impactor matter will become more widely and evenly disseminated, but we suggest that on the HED asteroid the only materials effectively homogenized (in the relative sense of siderophile-element variances) by a succession of impact-mixing episodes may be the high-Al_2O_3 howardites, and especially the regolithic howardites. By this scenario, it is possible (our limited sampling is frankly inadequate to test this; the polymict eucrite averages for Ni and Ir in Table 4 are skewed by one exceptionally siderophile-rich sample: EET 92023) that other types of HED polymict breccia contain, on *average*, nearly the same levels of siderophile enrichment as the high-Al_2O_3 howardites, the difference being that most of the siderophile-rich matter in the polymict eucrites and low-Al_2O_3 howardites is localized into a relative few isolated fragments that thus far, apart from EET 92023, have escaped detection.

4.4. Relative abundances of eucrite and diogenite

Ideally, to the degree that the impact-mixing process was random, the average composition of regolithic howardite may be used to constrain the relative proportions of eucrite and diogenite excavated on Vesta. The most useful elements for this purpose are those that are insensitive to "contamination" by meteoritic impact-debris (i.e., are lithophile, not siderophile), that show consistent large concentration disparity between diogenites and eucrites (including cumulate eucrites), and that are consistently well determined in our database. Elements satisfying these criteria include several major elements (MgO, Al_2O_3, CaO), the trace-compatible element V, and a variety of incompatible elements (e.g., Ti, La, Sm, Lu, Hf). For all these elements, the regolithic howardite composition (Table 4) is best fit by a mixture of 66–70 wt% average pristine-igneous eucrite with 30–34 wt% average pristine-igneous diogenite. The best constraints probably come from MgO, Al_2O_3 and CaO, all of which imply, for average regolithic howardite, a eucrite:diogenite mix ratio of precisely (to within 0.5%) 2:1. If instead the average overall howardite composition (Table 4) is modeled, the eucrite/diogenite mix ratio is implied to be more moderate, ~0.59. Even this would represent a substantial shift toward eucrite from early results such as those of Fukuoka et al. (1977), who found an average eucrite/diogenite mix ratio of 0.41 ± 0.10 for a set of eight howardites.

Unfortunately, because the impact-mixing process cannot be assumed random with respect to depth provenance, any such "unmixing" estimate is probably useful only as an upper limit for the actual eucrite/diogenite ratio on Vesta. Even before spectroscopic observations established that the largest, deepest basin on Vesta has an anomalously pyroxene-rich interior (Thomas et al., 1997), petrologists had inferred that most diogenite cumulates probably formed deeper than most eucrites (e.g., Takeda, 1979; Fowler et al., 1994; Mittlefehldt, 1994; Zema et al., 1997). Quantitatively, Grove and Bartels (1992) argued for diogenite petrogenesis at depth of order 130 km. Ruzicka et al. (1997) argued for origin in a layer just below the eucritic "upper crust," which they estimated (from Vesta's overall size, assuming efficient concentration of basalt out of a chondritic bulk composition) was roughly 25–40 km thick. Without a quantitative knowledge of the dimensions of the crater(s) that excavated the diogenitic materials (apart from the vestoid-forming impact, which is irrelevant for mixing materials into the pre-vestoid regolith) and of the compositional depth-layering within Vesta, we can only presume that the impact-excavation process that dumped lithic debris into the surface regolith probably, on average, oversampled the shallow eucrite component in relation to the deep diogenite component. The quantitative strength of this bias is guesswork; anything from a few tens of percent to a factor of two (or more) seems possible. Even so, given that the crudest unmixing model for the regolithic howardites (previous paragraph) implies 1/3 diogenite, the total diogenite/eucrite ratio on Vesta is probably (unless the shallow-eucrites, deep-diogenites model is completely fallacious) at least nearly one. As discussed by Warren (1985, 1997), as values for this ratio become $>>0.3$, larger and larger proportions of diogenite-related residual basaltic magma are implied to form; and in terms of sampled HEDs this implied residual basaltic magma must have become fractional-crystallization-produced eucrites, i.e., Nuevo Laredo trend eucrites.

4.5. Other aspects of Moon–Vesta analogy

The HED evidence may provide some lessons for lunar geochemistry. It is often assumed (e.g., Hertogen et al., 1977; Norman et al., 2002) that siderophile patterns of lunar impact-melt breccias can be diagnostic of the composition of the melt-generating impactor. But the Moon, like the HED asteroid, is a site of repeated impacts onto an unrecycled shallow interior. Although encounter velocities are not so gentle, a weaker but fundamentally similar potential may exist for the impactor debris from any individual impact to remain poorly disseminated. If so, the siderophile pattern found for any individual small chunk of impact melt formed relatively late in the lunar bombardment may reflect a mixture of debris scattered from prior great impacts in the same region, as much as, or even more than, it reflects the singular composition of the melt-generating impactor. Siderophile "signatures" are a valuable lunar-geochemical tool, but they should be interpreted, at least for young impactites, with caution.

The oldest components of the Moon's crust (as flotation products of the magma ocean) are probably the highly distinctive ferroan anorthosites (Warren, 2004; Norman et al., 2003). One of the largest, best-studied samples of this ancient rock type, 60025 (1.8 kg), is often considered pristine-igneous on the basis of extremely low siderophile levels (e.g., 6 pg/g Ir: Krähenbuhl et al., 1973). Yet when studied in detail and as a whole, 60025 appears polymict (James et al., 1991), even though all of its lithic components are some variety of ferroan anorthosite (so that the texture might be better described as genomict). We suggest that 60025 may be a lunar analog of the polymict eucrites, in the sense that it was brecciated only once (or at any rate not many times), and while still deep within a mass of essentially intact crust, which had not yet been pervasively contaminated by impactor-siderophile debris. As a result, 60025 represents the mixing of a detectable (albeit consistently ferroan-anorthositic) range of ancient lunar materials, yet without detectable incorporation of impactor debris.

The clustering of ages for lunar impact-melt breccias near 3.85 Ga is often (e.g., Norman et al., 2006) viewed as evidence for the cataclysm model of lunar cratering history, which postulates that a tremendous spike at $\sim 3.85 \pm 0.10$ Ga accounted for most of the total cratering since 4.4 Ga. This hypothesis is only plausible if the ~3.85-Ga cratering spike occurred throughout the inner solar system (and a dynamical model has recently been suggested to account for this: Gomes et al., 2005). Age data from HED breccias can thus provide an independent test; and in general, they have been broadly consistent with the cataclysm hypothesis (Bogard, 1995). However, in contrast with the Moon, older impact melts seem fairly common among HEDs. Yamaguchi et al. (2001) inferred that the impact "partial melting" of EET 90020 occurred at ~4.50 Ga. We (see the Electronic Annex) tentatively infer that PCA 91007 and 82502 are impact-melt products, and a K–Ar isotopic study by Bogard and Garrison (2001) found that both formed close to 4.5 Ga, and retain isotopic compositions "not significantly reset by late bombardment."

5. CONCLUSIONS

1. In many respects, our new analyses conform to a simple two-component (eucrite + diogenite) mixing trend for the polymict-HED breccias. Apart from siderophile elements (determined by the vagaries of impactor-debris admixture), the two-component model is least successful at accounting for incompatible element concentrations, mainly because pristine-igneous eucrites (including cumulates) are highly diverse for incompatible elements. Vanadium and Cr also, especially among MgO-rich howardites, display great scatter, traceable to diversity within the diogenites. A small component of cumulate eucrite in the howardites is confirmed by offset between the howardite Al_2O_3–MgO and CaO–Sc mixing trends (extrapolated) and the average composition of noncumulate eucrite. But very few, if any, of the analyzed howardites contain more cumulate than noncumulate eucrite.

2. Pristine-igneous HEDs feature extremely low siderophile levels, with enrichment in Ni/Ir by a relatively mild factor of ~2.5. This suggests near-complete partitioning of both Ni and Ir into the nascent core of the parent asteroid, an outcome that may require that the asteroid's deep interior was at one time mostly molten (cf. Righter and Drake, 1997).

3. Contrary to a popular misconception, howardites are generally not (at least, not in the sense normally employed in lunar petrology) regolith breccias. Most howardites are fragmental breccias; and their spectrum of Ni concentrations far more closely resembles that of lunar non-regolithic polymict impactites than it does that of lunar regolith breccias.

4. We propose that the howardites that truly are regolith breccias be distinguished as a distinct subclass: regolithic howardites. The most definitive characteristic of regolithic howardites is enrichment in solar-wind noble gases. But they are also distinctively rich in Ni (as convenient exemplar of highly siderophile elements), in glasses (especially spheroids and turbid-brown glass), and in impactor-chondritic clasts. In lunar petrology, regolith samples (including breccias) are valued (e.g., Warren et al., 2005) as very thorough blends of the crust focused, in a statistical yet highly systematic way, on the site of regolith accumulation. Regolithic howardites have a similar value, or an even greater one, considering that impact-mixing probably occurred at a more nearly global scale (in both the vertical as well as horizontal sense) on the relatively tiny HED asteroid.

5. The current set of four definite plus five probable regolithic howardites shows a remarkable clustering in major-element composition (or put another way, diogenite/eucrite ratio) near 8–9 wt% Al_2O_3; along with commensurate trace-lithophile characteristics (e.g., Cr clustering near 4.3 mg/g, Sm near 1.0 μg/g).

6. The high Ni contents of the regolithic howardites are part of a general trend among polymict HEDs, whereby Ni content is correlated with proximity of Al_2O_3 content to ~9 wt%. Polymict eucrites (mostly 11–13 wt% Al_2O_3) tend to be remarkably low in Ni, compared to all but the most Al_2O_3-poor howardites, or to any major type of lunar polymict material.

7. To account for the enigmatic clustering of regolithic howardite compositions near 8–9 wt% Al_2O_3, we suggest the addition of diogenite (deep pyroxenite) to the ancient crust transpired mainly as a result of a single early and exceptionally large impact, after which further shallow but laterally efficient mixing engendered a relatively uniform ~1:2 blend of diogenite:eucrite for the surface regolith. But most of the ancient regolith of Vesta, as represented by the regolithic howardites, was probably destroyed (largely dispersed, thoroughly buried) by a great impact that spalled off multiple vestoids >>5 km in diameter, probably within the last 1 Ga (Marzari et al., 1996). The modern regolith, accumulated since 1 Ga, may be very heterogeneous compared to the regolithic howardites.

8. The single-excavation model for ancient diogenite input may also help to explain the enigmatically low proportion of polymict diogenites. By this scenario, the diogenites were largely shielded from blending with dissimilar material until after their emplacement as pyroxenite fragments (up to multiple km in diameter, by analogy with the later vestoids) within a grossly howarditic surface ejecta layer.

9. The generally low Ni enrichment levels of the polymict eucrites and Al_2O_3-poor howardites may reflect inefficient dispersal of impactor debris during megagardening of the HED crust. Apparently, in the HED-asteroidal context (low collision velocities, etc.), only materials blended by multiple impacts consistently acquire major enrichments in siderophile elements.

10. Some large lunar ferroan anorthosite samples, such as 60025, may be analogously genomict yet siderophile-uncontaminated. Genomict yet "meteorite-free" brecciation was probably never common, but on the early Moon, before the lunar crust was "contaminated" on the scale of hundreds to thousands of meters, hand-sample scale genomict brecciation was probably more common (especially in deep-crustal settings) than it would be on the later, more mature Moon.

11. Taking solar noble gases as the most definitive test, the number of confirmed regolithic howardites is still small (4 or perhaps, including Malvern, 5); and our conclusions based on their populational characteristics are correspondingly tentative. Additional regolithic HEDs should be sought, by means of gas, petrographic, and siderophile measurements on howardites that are suggestively rich in glasses (e.g., Monticello: Olsen et al., 1987), or Ni (e.g., Muckera 001, LEW 85313, and perhaps even MAC 02666), or carbonaceous chondrite clasts (e.g., Y-793497: Gounelle et al., 2003).

ACKNOWLEDGMENTS

We thank D. Bogard, H. Palme and A. Ruzicka for insightful reviews, Associate Editor D. Mittlefehldt for additional helpful suggestions, George Miller for help with irradiations and short-half-life counting at UC-Irvine, and the sources listed in Tables 1–3 for generous donations of samples. This work was supported by NASA grant NAG5-12819.

APPENDIX A. SUPPLEMENTARY DATA

Supplementary data associated with this article can be found, in the online version, at doi:10.1016/j.gca.2009.06.030.

REFERENCES

Anand M., Taylor L. A., Neal C. R., Snyder G. A., Patchen A., Sano Y. and Terada K. (2003) Petrogenesis of lunar meteorite EET 86008. *Geochim. Cosmochim. Acta* **67**, 3499–3518.

Asphaug E. (1997) Impact origin of the Vesta family. *Meteor. Planet. Sci.* **32**, 965–980.

Barrat J. A., Jambon A., Bohn M., Blichert-Toft J., Sautter V., Göpel C., Gillet Ph., Boudouma O. and Keller F. (2003) Petrology and geochemistry of the unbrecciated achondrite North West Africa 1240 (NWA 1240): an HED parent body impact melt. *Geochim. Cosmochim. Acta* **67**, 3959–3970.

Barrat J. A., Yamaguchi A., Greenwood R. C., Bohn M., Cotten J., Benoit M. and Franchi I. A. (2007) The Stannern trend eucrites: contamination of main group eucritic magmas by crustal partial melts. *Geochim. Cosmochim. Acta* **71**, 4108–4124.

Barrat J. A., Bohn M., Gillet P. and Yamaguchi A. (2008a) Impact glasses in howardites: evidence for K-rich lithologies on 4 Vesta. *Lunar Planet. Sci.* **39** (abstr. 1589).

Barrat J. A., Yamaguchi A., Greenwood R. C., Benoit M., Cotten J., Bohn M. and Franchi I. A. (2008b) Geochemistry of diogenites: still more diversity in their parental melts. *Meteor. Planet. Sci.* **43**, 1759–1775.

Beck A. W., McSween, Jr., H. Y., Mittlefehldt D. W. and Lee C. A. (2009) Fused bead analysis in diogenite meteorites. *Lunar Planet. Sci.* **40** (abstr. 1177).

Binzel R. P. and Xu S. (1993) Chips off of asteroid 4 Vesta: evidence for the parent body of basaltic achondrite meteorites. *Science* **260**, 186–191.

Binzel R. P., Gaffey M. J., Thomas P. C., Zellner B. H., Storrs A. D. and Wells E. D. (1997) Geologic mapping of Vesta from Hubble Space telescope images. *Icarus* **128**, 95–103.

Bischoff A., Palme H., Weber H. W., Stöffler D., Braun O., Spettel B., Begemann F., Wänke H. and Ostertag R. (1987) Petrography, shock history, chemical composition and noble gas content of the lunar meteorites Yamato-82192 and -82193. *Proc. NIPR Sympos. Antarct. Met. (Tokyo)* **11**, 21–42.

Bischoff A., Scott E. R. D., Metzler K. and Goodrich C. A. (2006) Nature and origins of meteoritic breccias. In *Meteorites and the Early Solar System II* (eds. D. S. Lauretta and H. Y. McSween Jr.). University of Arizona Press, pp. 679–712.

Bjonnes E. E. and Delaney J. S. (2004) Constraints on the lithological variation near the surface of the HED planetoid from the petrology of 91 & 92 series Antarctic achondrites. *Lunar Planet. Sci.* **35** (abstr. 1030).

Bogard D. D. (1995) Impact ages of meteorites; a synthesis. *Meteoritics* **30**, 244–268.

Bogard D. D. and Garrison D. H. (2001) Early thermal history of eucrites by ^{39}Ar–^{40}Ar. *Lunar Planet. Sci.* **32** (abstr. 1138).

Bowman L. E., Papike J. J. and Spilde M. N. (1999) Diogenites as asteroidal cumulates: insights from spinel chemistry. *Am. Mineral.* **84**, 1020–1026.

Buchanan P. C., Zolensky M. E. and Reid A. M. (1993) Carbonaceous chondrite clasts in the howardites Bholghati and EET 87513. *Meteoritics* **28**, 659–682.

Burbine T. H., Buchanan P. C., Binzel R. P., Bus S. J., Hiroi T., Hinrichs J. L., Meibom A. and McCoy T. J. (2001) Vesta, Vestoids, and the howardite, eucrite, diogenite group: relationships and the origin of spectral differences. *Meteor. Planet. Sci.* **36**, 761–781.

BVSP (1981) *Basaltic Volcanism on the Terrestrial Planets*, Pergamon, p. 1286.

Carlson R. W. and Lugmair G. W. (2000) Timescales of planetesimal formation and differentiation based on extinct and extant radioisotopes. In *Origin of the Earth and Moon* (eds. R. M. Canup and K. Righter). University of Arizona Press, pp. 25–44.

Chou C. L., Boynton W. V., Bild R. W., Kimberlin J. and Wasson J. T. (1976) Trace element evidence regarding a chondritic component in howardite meteorites. *Proc. Lunar Sci. Conf.* **7**, 3501–3518.

Davis D. R., Chapman C. R., Greenberg R. and Weidenschilling S. J. (1979) Collisional evolution of asteroids: populations, rotations, and velocities. In *Asteroids* (ed. T. Gehrels). Univ. Arizona, pp. 528–557.

Delaney J. S., Takeda H., Prinz M., Nehru C. E. and Harlow G. E. (1983) The nomenclature of polymict basaltic achondrites. *Meteoritics* **18**, 103–111.

Delaney J. S., Prinz M. and Takeda H. (1984) The polymict eucrites. *Proc. Lunar Planet. Sci. Conf.* **15**, C251–C288.

Delano J. W., Zellner N. E. B., Barra F., Olson E., Swindle T. D., Tibbetts N. J. and Whittet D. C. B. (2007) An integrated approach to understanding Apollo 16 impact glasses: chemistry, isotopes, and shape. *Meteor. Planet. Sci.* **42**, 993–1004.

Dreibus G., Kruse H., Spettel B. and Wänke H. (1977) The bulk composition of the Moon and the eucrite parent body. *Proc. Lunar Sci. Conf.* **8**, 211–227.

Farinella P. and Davis D. R. (1992) Collision rates and impact velocities in the main asteroid belt. *Icarus* **97**, 111–123.

Fowler G. W., Papike J. J., Spilde M. N. and Shearer C. K. (1994) Diogenites as asteroidal cumulates: insights from orthopyroxene major and minor element chemistry. *Geochim. Cosmochim. Acta* **58**, 3921–3929.

Frost M. J. (1971) The Molteno meteorite. *Mineral. Mag.* **38**, 89–93.

Fuhrman M. and Papike J. J. (1981) Howardites and polymict eucrites: regolith samples from the eucrite parent body: petrology of Bholgati, Bununu, Kapoeta, and ALHA76005. *Proc. Lunar Planet. Sci. Conf.* **12**, 1257–1279.

Fukuoka T., Boynton W. V., Ma M. S. and Schmitt R. A. (1977) Genesis of howardites, diogenites, and eucrites. *Proc. Lunar Sci. Conf.* **8**, 187–210.

Gaffey M. J. (1997) Surface lithologic heterogeneity of asteroid 4 Vesta. *Icarus* **127**, 130–157.

Gardner K. G. and Mittlefehldt D. W. (2004) Petrology of new Stannern-trend eucrites and eucrite genesis. *Lunar Planet. Sci.* **35** (abstr. 1349).

Gomes R., Levison H. F., Tsiganis K. and Morbidelli A. (2005) Origin of the cataclysmic Late Heavy Bombardment period of the terrestrial planets. *Nature* **435**, 466–469.

Gounelle M., Zolensky M. E., Liou J.-C., Bland P. A. and Alard O. (2003) Mineralogy of carbonaceous chondritic microclasts in howardites: identification of C2 fossil micrometeorites. *Geochim. Cosmochim. Acta* **67**, 507–527.

Govindaraju K. (1994) 1994 compilation of working values and sample description for 383 geostandards. *Geostan. Newsl.* **18**, 1–158.

Greshake A., Schmitt R. T., Stöffler D., Pätsch M. and Schultz L. (2001) Dhofar 081: a new lunar highland meteorite. *Meteor. Planet. Sci.* **36**, 459–470.

Grossman J. N. (2000) The meteoritical bulletin, no. 84, 2000 August. *Meteor. Planet. Sci.* **35**(Suppl.), A199–A225.

Grossman J. N. and Baedecker P. N. (1986) Computer graphics for quality control in the INAA of geological samples. In *Proc. 7th Intl. Conf. on Modern Trends in Activation Analysis*, pp. 571–578.

Grove T. L. and Bartels K. S. (1992) The relation between diogenitic cumulates and eucrite magmas. *Proc. Lunar Planet. Sci.* **22**, 437–445.

Hardersen P. S., Gaffey M. J. and Abell P. A. (2004) Mineralogy of Asteroid 1459 Magnya and implications for its origin. *Icarus* **167**, 170–177.

Haskin L. A. and Warren P. H. (1991) Chemistry. In *Lunar Sourcebook, A User's Guide to the Moon* (eds. G. Heiken, D. Vaniman and B. M. French). Cambridge Univ. Press, pp. 357–474.

Hertogen J., Janssens M. J., Takahashi H., Palme H. and Anders E. (1977) Lunar basins and craters: evidence for compositional changes of bombarding population. *Proc. Lunar Sci. Conf.* **8**, 17–45.

Hewins R. H. (1982) The origin of achondrite breccias (abstract). In *Workshop on Lunar Breccias and Soils and their Meteoritic Analogs* (eds. G. J. Taylor and L. L. Wilkening). Lunar and Planetary Institute, pp. 44–48.

Housen K. R. and Wilkening L. L. (1982) Regoliths on small bodies in the solar system. *Ann. Rev. Earth Planet. Sci.* **10**, 355–376.

James O. B., Lindstrom M. M. and McGee J. J. (1991) Lunar ferroan anorthosite 60025: petrology and chemistry of mafic lithologies. *Proc. Lunar Planet. Sci. Conf.* **21**, 63–87.

Jerome D. Y. (1970) Composition and origin of some achondritic meteorites. Ph. D. thesis, Univ. Oregon, Eugene.

Jerome D. Y. and Goles G. G. (1971) A re-examination of relationships among pyroxene-plagioclase achondrites. In *Activation Analysis in Geochemistry and Cosmochemistry* (eds. A. O. Brunfelt and E. Steinnes). Universitetsforlaget, pp. 261–266.

Jochum K. P., Grais K. I. and Hintenberger H. (1980) Chemical composition and classification of 19 Yamato meteorites. *Meteoritics* **15**, 31–39.

Kallemeyn G. W. (1993) Neutron activation analysis. In *Advances in Analytical Chemistry* (eds. M. Hyman and M. W. Rowe). JAI Press, pp. 193–209.

Keil K. (2002) Geological history of asteroid 4 Vesta: the "Smallest Terrestrial Planet". In *Asteroids III* (eds. W. F. Bottke Jr., A. Cellino, P. Paolicchi and R. P. Binzel). University of Arizona, pp. 573–584.

Kelley M. S., Vilas F., Gaffey M. J. and Abell P. A. (2003) Quantified mineralogical evidence for a common origin of 1929 Kollaa with 4 Vesta and the HED meteorites. *Icarus* **165**, 215–218.

Kirsten T. and Horn P. (1977) ^{39}Ar–^{40}Ar dating of basalts and rock breccias from Apollo 17 and the Malvern achondrite. In *The Soviet-American Conference on Cosmochemistry of the Moon and Planets* (eds. J. H. Pomeroy and N. J. Hubbard). NASA SP-370, pp. 525–540.

Kluger F., Weinke H. and Kiesl W. (1983) Chondrule formation by impact? The cooling rate. In *Chondrules and Their Origins* (ed. E. King). Lunar Planet. Institute, pp. 188–194.

Korotev R. L. (1987) The nature of the meteoritic components of Apollo 16 soil, as inferred from correlations of iron, cobalt, iridium, and gold with nickel. *Proc. Lunar Planet. Sci. Conf.* **17**, E447–E461.

Krähenbuhl U., Ganapathy R., Morgan J. W. and Anders E. (1973) Volatile elements in Apollo 16 samples: implications for highland volcanism and accretion history of the Moon. *Proc. Lunar Sci. Conf.* **4**, 1325–1348.

Kurat G., Varela M. E., Zinner E., Maruoka T. and Brandstätter F. (2003) Major, minor and trace elements in some glasses from the NWA 1664 howardite. *Lunar Planet. Sci.* **34** (abstr. 1733).

Laul J. C., Keays R. R., Ganapathy R., Anders E. and Morgan J. W. (1972) Chemical fractionations in meteorites – V. Volatile and siderophile elements in achondrites and ocean ridge basalts. *Geochim. Cosmochim. Acta* **36**, 329–345.

Lorenz K. A., Nazarov M. A., Kurat G., Brandstätter F. and Ntaflos T. (2007) Foreign meteoritic material of howardites and polymict eucrites. *Petrologiya* **15**, 115–132.

Lorenzetti S., Busemann H. and Eugster O. (2005) Regolith history of lunar meteorites. *Meteor. Planet. Sci.* **40**, 315–327.

Lucey P., Korotev R. L., Gillis J. J., Taylor L. A., Lawrence D., Campbell B. A., Elphic R., Feldman B., Hood L. L., Hunten D., Mendillo M., Noble S., Papike J. J., Reedy R. C., Lawson

S., Prettyman T., Gasnault O. and Maurice S. (2006) Understanding the lunar surface and space-moon interactions. In *New Views of the Moon*, vol. 60 (eds. B. L. Jolliff, M. A. Wieczorek, C. K. Shearer and C. R. Neal). Mineral. Soc. Am. Rev. Mineral. Geochem., pp. 83–219.

Marzari F., Cellino A., Davis D. R., Farinella P., Zappala V. and Vanzani V. (1996) Origin and evolution of the Vesta asteroid family. *Astron. Astrophys.* **316**, 248–262.

Mason B. (1983) The definition of a howardite. *Meteoritics* **18**, 245.

Mayne R. G., McSween, Jr., H. Y., McCoy T. J. and Gale A. (2009) Petrology of the unbrecciated eucrites. *Geochim. Cosmochim. Acta* **73**, 794–819.

McCarthy T. S., Ahrens L. H. and Erlank A. J. (1972) Further evidence in support of the mixing model for howardite origin. *Earth Planet. Sci. Lett.* **15**, 86–93.

McKay D. S., Bogard D. D., Morris R. V., Korotev R. L., Johnson P. and Wentworth S. J. (1986) Apollo 16 regolith breccias: characterization and evidence for early formation in the megaregolith. *Proc. Lunar Planet. Sci. Conf.* **16**, D277–D303.

McKay D. S., Heiken G., Basu A., Blanford G., Simon S., Reedy R., French B. M. and Papike J. (1991) The lunar regolith. In *Lunar Sourcebook, A User's Guide to the Moon* (eds. G. H. Heiken, D. T. Vaniman and B. M. French). Cambridge Univ. Press, pp. 285–356.

Mittlefehldt D. W. (1979) Petrographic and chemical characterization of igneous lithic clasts from mesosiderites and howardites and comparison with eucrites and diogenites. *Geochim. Cosmochim. Acta* **43**, 1917–1935.

Mittlefehldt D. W. (1994) The genesis of diogenites and HED parent body petrogenesis. *Geochim. Cosmochim. Acta* **58**, 1537–1552.

Mittlefehldt D. W. (2005) Ibitira: a basaltic achondrite from a distinct parent asteroid and implications for the Dawn mission. *Meteor. Planet. Sci.* **40**, 665–677.

Mittlefehldt D. W. and Lindstrom M. M. (2003) Geochemistry of eucrites: genesis of basaltic eucrites, and Hf and Ta as petrogenetic indicators for altered Antarctic eucrites. *Geochim. Cosmochim. Acta* **67**, 1911–1935.

Norman M. D., Bennett V. C. and Ryder G. (2002) Targeting the impactors: siderophile element signatures of lunar impact melts from Serenitatis. *Earth Planet. Sci. Lett.* **202**, 217–228.

Norman M. D., Borg L., Nyquist L. E. and Bogard D. D. (2003) Chronology, geochemistry, and petrology of a ferroan noritic anorthosite clast from Descartes breccia 67215: clues to the age, origin, structure, and impact history of the lunar crust. *Meteor. Planet. Sci.* **38**, 645–661.

Norman M. D., Duncan R. A. and Huard J. J. (2006) Identifying impact events within the lunar cataclysm from ^{40}Ar–^{39}Ar ages and compositions of Apollo 16 impact melt rocks. *Geochim. Cosmochim. Acta* **70**, 6032–6049.

Nyquist L. E., Bogard D. D., Shih C.-Y., Greshake A., Stöffler D. and Eugster O. (2001) Ages and geologic histories of martian meteorites. *Space Sci. Rev.* **96**, 105–164.

Olsen E. J., Dod B. D., Schmitt R. A. and Sipiera P. P. (1987) Monticello: a glass-rich howardite. *Meteoritics* **22**, 81–96.

Olsen E. J., Fredriksson K., Rajan S. and Noonan A. (1990) Chondrule-like objects and brown glasses in howardites. *Meteoritics* **25**, 187–194.

Palme H., Spettel B., Burghele A., Weckwerth G. and Wänke H. (1983) Elephant Moraine polymict eucrites: a eucrite-howardite compositional link. *Lunar Planet. Sci.* **14**, 590–591.

Patzer A., Schultz L. and Franke L. (2003) New noble gas data of primitive and differentiated achondrites including Northwest Africa 011 and Tafassasset. *Meteor. Planet. Sci.* **38**, 1485–1497.

Richardson, Jr., J. E., Melosh H. J., Greenberg R. J. and O'Brien D. P. (2005) The global effects of impact-induced seismic activity on fractured asteroid surface morphology. *Icarus* **179**, 325–349.

Righter K. and Drake M. J. (1997) A magma ocean on Vesta: core formation and petrogenesis of eucrites and diogenites. *Meteor. Planet. Sci.* **32**, 929–944.

Rubin A. E. (1997) The Hadley Rille enstatite chondrite and its agglutinate-like rim: impact melting during accretion to the Moon. *Meteor. Planet. Sci.* **32**, 135–141.

Ruzicka A., Snyder G. A. and Taylor L. A. (1997) Vesta as the HED parent body: implications for size of a core and for large-scale differentiation. *Meteor. Planet. Sci.* **32**, 825–840.

Shearer C. K., Fowler G. W. and Papike J. J. (1997) Petrogenetic models for magmatism on the eucrite parent body: evidence from orthopyroxene in diogenites. *Meteor. Planet. Sci.* **32**, 877–889.

Shukolyukov Y. A., Nazarov M. A., Pätsch M. and Schultz L. (2001) Noble gases in three lunar meteorites from Oman. *Lunar Planet. Sci.* **32** (abstr. 1502).

Sisodia M. S., Shukla A. D., Suthar K. M., Mahajan R. R., Murty S. V. S., Shukla P. N., Bhandari N. and Natarajan R. (2001) The Lohawat howardite: mineralogy, chemistry and cosmogenic effects. *Meteor. Planet. Sci.* **36**, 1457–1466.

Takeda H. (1979) A layered-crust model of a howardite parent body. *Icarus* **40**, 455–470.

Takeda H., Miyamoto M., Mori H., Wentworth S. J. and McKay D. S. (1990) Mineralogical comparison of the Y86032-type lunar meteorites to feldspathic fragmental breccia 67016. *Proc. Lunar Planet. Sci. Conf.* **20**, 91–100.

Thomas P. C. (1999) Large craters on small objects: occurrence, morphology, and effects. *Icarus* **142**, 89–96.

Thomas P. C., Binzel R. P., Gaffey M. J., Storrs A. D., Wells E. N. and Zellner B. H. (1997) Impact excavation on asteroid 4 Vesta: Hubble Space telescope results. *Science* **277**, 1492–1495.

Usui T. and McSween, Jr., H. Y. (2007) Geochemistry of 4 Vesta based on HED meteorites: prospective study for interpretation of gamma ray and neutron spectra for the Dawn mission. *Meteor. Planet. Sci.* **42**, 255–269.

Vogt S., Herzog G. F., Eugster O., Michel T., Niedermann S., Krähenbuhl U., Middleton R., Dezfouly-Arjomandy B., Fink D. and Klein J. (1993) Exposure history of the lunar meteorite, Elephant Moraine 87521. *Geochim. Cosmochim. Acta* **57**, 3793–3799.

Walton J. R., Lakatos S. and Heymann D. (1973) Distribution of inert gases in fines from the Cayley-Descartes region. *Proc. Lunar Sci. Conf.* **4**, 2079–2095.

Warren P. H. (1985) Origin of howardites, diogenites and eucrites: a mass balance constraint. *Geochim. Cosmochim. Acta* **49**, 577–586.

Warren P. H. (1997) MgO–FeO mass balance constraints and a more detailed model for the relationship between eucrites and diogenites. *Meteor. Planet. Sci.* **32**, 945–963.

Warren P. H. (2004) The Moon. In *Treatise on Geochemistry, Volume 1, Meteorites, Comets, and Planets* (ed. A. M. Davis). Elsevier, pp. 559–599.

Warren P. H. and Gessler P. (2001) Bluewing 001: a new eucrite with extremely unequilibrated pyroxene, cognate (?) eucritic xenoliths, and Stannern-like geochemistry. *Lunar Planet. Sci.* **32** (abstr. 1970).

Warren P. H. and Jerde E. (1987) Composition and origin of Nuevo Laredo Trend eucrites. *Geochim. Cosmochim. Acta* **51**, 713–725.

Warren P. H. and Kallemeyn G. W. (1989) Elephant moraine 87521: the first lunar meteorite composed of predominantly mare material. *Geochim. Cosmochim. Acta* **53**, 3323–3330.

Warren P. H., Jerde E. A., Migdisova L. F. and Yaroshevsky A. A. (1990) Pomozdino: an anomalous, high MgO/FeO, yet REE-rich eucrite. *Proc. Lunar Planet. Sci. Conf.* **20**, 281–297.

Warren P. H., Kallemeyn G. W. and Kyte F. T. (1999) Origin of planetary cores: evidence from highly siderophile elements in martian meteorites. *Geochim. Cosmochim. Acta* **63**, 2105–2122.

Warren P. H., Ulff-MØller F. and Kallemeyn G. W. (2005) "New" lunar meteorites: impact melt and regolith breccias and large-scale heterogeneities of the upper lunar crust. *Meteor. Planet. Sci.* **40**, 989–1014.

Warren P. H., Ulff-MØller F., Huber H. and Kallemeyn G. W. (2006) Siderophile geochemistry of ureilites: a record of early stages of planetesimal core formation. *Geochim. Cosmochim. Acta* **70**, 2104–2126.

Wasson J. T. and Kallemeyn G. W. (1988) Compositions of chondrites. *Philos. Trans. R. Soc. London A* **325**, 535–544.

Wasson J. T., Chapman C. R., Grogan K. and Dermott S. F. (1996) Possible formation of the Vesta-family asteroids and the main IRAS dust band by an oblique impact on Vesta (abstract). *Lunar Planet. Sci.* **27**, 1387–1388.

Welten K. C., Lindner L., van der Borg K., Loeken T., Scherer P. and Schultz L. (1997) Cosmic-ray exposure ages of diogenites and the recent collisional history of the howardite, eucrite and diogenite parent body/bodies. *Meteor. Planet. Sci.* **32**, 891–902.

Wiechert U. H., Halliday A. N., Palme H. and Rumble D. (2004) Oxygen isotope evidence for rapid mixing of the HED meteorite parent body. *Earth Planet. Sci. Lett.* **221**, 373–382.

Wolf R., Ebihara M., Richter G. R. and Anders E. (1983) Aubrites and diogenites: trace element clues to their origins. *Geochim. Cosmochim. Acta* **47**, 2257–2270.

Wolf D., Palme H. and Zipfel J. (2001) The bulk chemical compositions of eucrites, polymict eucrites, howardites and diogenites. *Meteor. Planet. Sci.* **36**, A225.

Yamaguchi A., Taylor G. J., Keil K., Floss C., Crozaz G., Nyquist L. E., Bogard D. D., Garrison D. H., Reese Y. D., Weismann H. and Shih C.-Y. (2001) Post-crystallization reheating and partial melting of eucrite EET 90020 by impact into the hot crust of asteroid 4Vesta 4.50 Ga ago. *Geochim. Cosmochim. Acta* **65**, 3577–3599.

Yanai K. and Kojima H. (1995) *Catalog of the Antarctic Meteorites*. National Institute of Polar Research, p. 230.

Zahnle K. J. (2006) Earth's earliest atmosphere. *Elements* **2**, 217–222.

Zema M., Domeneghetti M. C., Molin G. M. and Tazzoli V. (1997) Cooling rates of diogenites: a study of Fe^{2+}–Mg ordering in orthopyroxene by single-crystal X-ray diffraction. *Meteor. Planet. Sci.* **32**, 855–862.

Zolensky M., Weisberg M. K., Buchanan P. C. and Mittlefehldt D. W. (1996) Mineralogy of carbonaceous chondrite clasts in HED achondrites and the Moon. *Meteor. Planet. Sci.* **31**, 518–537.

Associate editor: David W. Mittlefehldt